Air Force Institute of Technology
AFIT Scholar

Theses and Dissertations | Student Graduate Works

6-2007

High Temperature Degradation of 5250-4 Polymer Resin

Patrick E. Link

Follow this and additional works at: https://scholar.afit.edu/etd

 Part of the Aerospace Engineering Commons, and the Polymer and Organic Materials Commons

Recommended Citation

Link, Patrick E., "High Temperature Degradation of 5250-4 Polymer Resin" (2007). *Theses and Dissertations*. 2943.
https://scholar.afit.edu/etd/2943

This Thesis is brought to you for free and open access by the Student Graduate Works at AFIT Scholar. It has been accepted for inclusion in Theses and Dissertations by an authorized administrator of AFIT Scholar. For more information, please contact richard.mansfield@afit.edu.

HIGH TEMPERATURE DEGRADATION OF 5250-4 POLYMER RESIN

THESIS

Patrick E. Link, Ensign, USN

AFIT/GAE/ENY/07-J12

DEPARTMENT OF THE AIR FORCE
AIR UNIVERSITY

AIR FORCE INSTITUTE OF TECHNOLOGY

Wright-Patterson Air Force Base, Ohio

APPROVED FOR PUBLIC RELEASE; DISTRIBUTION UNLIMITED

The views expressed in this thesis are those of the author and do not reflect the official policy or position of the United States Air Force, Department of Defense, or the United States Government.

AFIT/GAE/ENY/07-J12

HIGH TEMPERATURE DEGRADATION OF 5250-4 POLYMER RESIN

THESIS

Presented to the Faculty

Department of Aeronautical and Astronautical Engineering

Graduate School of Engineering and Management

Air Force Institute of Technology

Air University

Air Education and Training Command

In Partial Fulfillment of the Requirements for the

Degree of Master of Science in Aeronautical Engineering

Patrick E. Link

Ensign, USN

June 2007

APPROVED FOR PUBLIC RELEASE; DISTRIBUTION UNLIMITED.

AFIT/GAE/ENY/07-J12

HIGH TEMPERATURE DEGRADATION OF 5250-4 POLYMER RESIN

Patrick E. Link
Ensign, USN

Approved:

//SIGNED//	
Dr. Anthony N. Palazotto (Chairman)	Date
//SIGNED//	
Dr. Greggory A. Schoeppner (Member)	Date
//SIGNED//	
Dr. Marina B. Ruggles-Wrenn (Member)	Date

Abstract

5250-4 bismaleimide resin is used in high performance polymer matrix composites with high temperature aeronautical applications. This thesis investigated the thermal and oxidative degradation of 5250-4 neat resin powder in argon, air, and oxygen environments. The powder was aged at 163^{0}C, 177 ^{0}C, and 190^{0}C in all environments for at least 250 hours. Isothermal thermo-gravimetric analysis demonstrated that weight loss was negligible for aging in the argon environment, indicating weight loss is the result of an oxidative process at these temperatures. The 5250-4 powder exhibited an initial period of weight gain before eventually losing weight in both air and oxygen. The applicability of a closed loop oxidation scheme to 5250-4 gravimetric behavior was investigated. Kinetic parameters for the scheme were determined for the Air Force Research Laboratory's polymer matrix composite lifetime prediction modeling efforts.

Acknowledgements

I would like to thank my thesis advisor, Dr. Palazotto for the guidance and support offered throughout this project. I would also like to thank the sponsor of this research, Dr. Greg Schoeppner , for the for the resources and direction he contributed to my efforts. In addition, I would like to thank Bill Price and Tara Storage for the technical support necessary to complete my experiments in the limited time available.

Patrick E. Link

Table of Contents

Page

List of Figures

Page

Page

List of Tables

Page

HIGH TEMPERATURE DEGRADATION OF 5250-4 POLYMER RESIN

I. Introduction and Literature Review

Background

Composite materials can achieve high specific stiffness and strengths by coupling the mechanical properties of strong fiber materials with relatively low weight matrix materials. The matrix material acts to hold the fiber in the desired orientation, while the fiber makes the composite much stronger than the matrix would be by itself. The high strength to weight of composites continues to increase their use in the field of aeronautical engineering. By reducing aircraft weight, the use of polymer matrix composites can result in increased range, reduced fuel consumption, higher payload capability, and increased maneuverability.

Today, polymer matrix composites are used extensively in the aircraft industry for engine components and skins of supersonic aircraft. Aromatic polyimides have proven especially useful for these applications because of their thermal and oxidative stability (1). As new high temperature polymer matrix composites are developed with higher service temperatures, a larger portion of high temperature components can be made of weight saving composites, therefore increasing the performance of the aircraft. Indeed, the difference in weight fraction of composites to total weight in the F/A-18A (~5%) and the JSF (~35%) demonstrate advances in the field of polymer science (2: 2).

A major problem in the aeronautical design process, however, is qualifying a new material for a given use. This has been a significant barrier to entry for new polymer matrix composites in aeronautical applications. Currently, the certification process involves expensive and time consuming experiments in which a composite is exposed to extreme conditions for extended periods of time. Material properties such as strength, toughness, and durability are then tested against industry standards. This trial and error method is extremely impractical considering the many material combinations of matrix and fiber that are involved in polymer matrix composite development (3). The cost of this process may encourage some designers to rely on previously proven materials rather than spending the time and money to determine if a newer material is as good or even better suited for the application (4).

This is the motivation behind the Air Force Research Laboratories' efforts to develop a life-performance prediction modeling capability. The ability to predict the degradation of a polymer matrix composite, rather than relying solely on experimentation, can save time and money. Barriers to entry of new polymer matrix composites for aircraft design will therefore be diminished. To develop this type of prediction capability, it is necessary to use a mechanistic model in which significant chemical processes of degradation are identified to predict lifetime performance of a polymer matrix composite.

According to McManus et al, the ideal mechanistic model could predict long-term mechanical properties based solely on the chemical composition of a particular material (3). However, the complexity of the reactions involved in polymer matrix composite degradation makes this approach impossible. For example, once the polymer matrix

begins to degrade, it can become a completely new material, with a new chemical structure, and a new set of chemical reactions with the environment. Therefore, it is still common practice to build a mechanistic model based on experimental observations of how a polymer changes in different environments. Doing so can help determine the pertinent aging mechanisms a polymer matrix composite will encounter throughout its lifetime of service.

Aging Mechanisms

Aging in this thesis is defined as the modification of a material's structure which negatively impacts material properties. This broad definition includes a wide range of processes. The first step in developing a modeling capability is to understand the many complex aging mechanisms and how they interact with each other. By determining which mechanisms are responsible for a particular outcome, the behavior of the material in a specified environment can be predicted. The aging mechanisms of high temperature polymer matrix composites can be separated into two main categories: physical aging and chemical aging.

Physical aging is the process of the material moving to its equilibrium state. When the temperature of an amorphous solid is below its glass transition temperature, its volume, enthalpy, and entropy are generally greater than their equilibrium values (5). In a sense, the material is frozen in a thermodynamic state which is not at its lowest energy. Physical aging refers to the changes in the organization of the polymer, without changing the chemical structure, which bring the material closer to its equilibrium. This process, also known as structural relaxation, can degrade the material by eliminating the beneficial

properties of the polymer's original conformation. This type of polymer aging is usually considered thermodynamically reversible. Although in practice, thermoset polymer matrix composites that undergo physical aging cannot always be restored to their original state.

Chemical aging refers to the irreversible change in the chemical structure of the polymer. Structural changes can result from chain scission (the breaking of skeletal bonds) or increases or decreases in crosslink density (6: 423). An example of chemical aging is thermo-oxidative aging, where the polymer reacts with oxygen in the atmosphere. Chemical aging does not need such an atmospheric interaction, however. An increase in temperature alone can also cause irreversible changes to a polymer's chemical structure. Such chemical dissociation resulting from heat is called thermolysis. Oxidation, however, is the primary chemical degradation mechanism in polymer matrix composites (7). It is especially important to consider in aeronautical applications, where hot, oxidative environments are commonly encountered. Thermo-oxidative aging is therefore investigated in this thesis.

Accelerated Aging

For polymer matrix composites used in aeronautical applications, aging occurs over the course of many years. Testing a polymer at its use conditions is therefore time consuming and impractical. A material is often aged at more severe conditions, such as at a higher temperature or higher oxygen partial pressure, in order to observe its aging characteristics in a shorter period of time. The aging behavior for the accelerated test

must then be correlated to the lifetime performance of the material at its service conditions.

Careful consideration must be given to the selection of test conditions for accelerated aging experiments. At higher temperatures, the aging mechanisms of a polymer might be significantly different than those observed at the polymer's service temperature. One reason for this is the additional cross-linking that occurs in the polymer at higher temperatures (4). Alternatively, increasing the partial pressure of oxygen is a method of accelerating oxidation without changing the temperature dependent oxidative mechanisms.

The partial pressure of oxygen refers to the portion of total pressure in a gas contributed by oxygen. For example, the partial pressure of oxygen in air is approximately 21% of the total pressure of the air. Therefore, to increase the partial pressure of oxygen for accelerated aging, either the total pressure of air can be increased, or gas with a higher oxygen content can be used. Higher partial pressures of oxygen promote greater rates of oxidation because oxidation increases with oxygen concentration in the polymer, which according to Henry's law is equal to the product of solubility and partial pressure.

As polymers age, many material properties such as modulus, toughness and density can change. Any of these properties can be used as a metric for aging. However, in most cases the easiest aging phenomena to observe in accelerated aging tests is weight loss. For this reason, thermo-gravimetric analysis is often used to characterize thermal degradation. The weight loss of the polymer must then be correlated with the material properties of interest in design.

Thermo-gravimetric analysis can be used in relating the weight of the polymer to temperature and time. In dynamic thermo-gravimetric analysis, the weight of a polymer is continuously measured while the polymer is subjected to a specified temperature profile, producing a weight versus temperature curve. Isothermal thermo-gravimetric analysis entails measuring the weight of the polymer as it is aged at a constant temperature, producing a weight versus time curve. Conducting isothermal thermo-gravimetric analysis at several temperatures produces a series of curves, from which the dependence of weight loss on time and temperature can be evaluated.

Time Temperature Equivalence

Time temperature equivalence is a concept often associated with viscoelastic theory used to describe the accelerated aging effects that elevated temperatures have on certain material properties. Applied to weight loss, this method can be used to develop weight loss versus time curves at temperatures that were not actually tested.

With isothermal thermo-gravimetric analysis of bismaleimide and epoxy composites in air, Seferis (8) demonstrated that the concept of equivalent property time (EPT) is useful for representing gravimetric curves produced by plotting weight as a function of time. With EPT, if the time necessary for a polymer to reach a particular conversion state (i.e. weight loss) at a given reference temperature is known, then the time needed for the polymer to reach that same conversion at a different temperature can be calculated. The derivation for this method is outlined in the *Theory* section.

The concept of EPT requires the activation energy of the weight loss process to be independent of temperature within the domain of interest. This means that the energy that must be applied to the system in order to start the conversion cannot be temperature

dependent. Seferis observes that for the bismalemide tested, the activation energy below 340^0C is different than the activation energy above 350^0C. This suggests different mechanisms are responsible for weight loss for the two different temperature domains. Therefore, a different activation energy and a different reference time are needed to calculate the EPT for temperatures above and below the 340^0C boundary.

While methods such as equivalent property time are useful for interpolating gravimetric curves for different temperatures than those tested, such methods do not offer much insight into the phenomena governing the gravimetric curves. More information about the degradation process can be evaluated with a kinetic model. Some examples of simple kinetic models are examined in the subsequent section.

Simple Kinetic Models

Regnier and Guibe (1) performed dynamic thermo-gravimetric analysis on KERIMID 736 (K736) bismaleimide resin at several heating rates in air and in nitrogen. A single weight loss stage was observed in a nitrogen atmosphere and two distinct stages in air, indicating the polymer degradation in air is the result of multiple mechanisms operating simultaneously. A simple model was then used to describe the BMI weight loss with only three parameters.

In order to construct a model for this weight loss, Regnier and Guibe used the following definition of conversion:

$$a=\frac{M_0-M}{M_0-M_f} \tag{1}$$

where M is mass, M_0 is initial mass, and M_f is final mass. The rate of degradation was defined as follows:

$$\frac{da}{dt}=kf(a) \tag{2}$$

where k is a temperature dependent rate constant given by the Arrhenius relation

$$k=A\exp\left(\frac{-E}{RT}\right) \tag{3}$$

where E is activation energy, R is the gas constant, and T is temperature. Regnier and Guibe (1) then used a power law relationship to model the rate of degradation:

$$f(a)=(1-a)^n \tag{4}$$

Several methods for determining the kinetics parameters (E, A, f(a)) from dynamic thermogravimetry were evaluated. Each method produced similar results, but it was decided that isothermal thermo-gravimetric analysis was better suited for finding true kinetics parameters.

It must be pointed out that this type of kinetic model assumes that activation energy is constant with respect to conversion. According to Budrugeac (9), activation energy often is not independent of conversion. This situation requires solving for multiple sets of parameters, each of which would be applicable to a certain range of weight loss.

Rodriguez-Arnold et al conducted isothermal thermo-gravimetric analysis to determine the Arrhenius parameters E and A as well as the form of the model f(α) for PX1000 and PX1200 polymers (10). The same general expression (equation 2) was used for the rate of conversion. They first separated variables and integrated equation 2 to obtain

$$g(a)=\int_0^a \frac{da}{f(a)}=k(T)\int_0^t dt \tag{5}$$

substituting the Arrhenius expression in for k results in

$$g(a)=Ae^{\left(\frac{-E_a}{RT}\right)}t \tag{6}$$

where the left hand side is a function of conversion (a) and the right hand side is a function of time. They found that the form of g(a) that best represented the weight loss data for aging the polymers in air at constant temperature in the range of 400^0C-500^0C was given by the Prout-Tompkins model:

$$g(a)=\ln\left(\frac{a}{1-a}\right) \tag{7}$$

This model represents autocatalytic decomposition, meaning that a product of the reaction is a catalyst or initiator of the reaction (10). The model was not a good representation of the isothermal data in a nitrogen atmosphere however. This means that oxidation is probably responsible for the autocatalytic behavior of the polymer weight loss. A closer investigation of the oxidative process can help to explain this self accelerating behavior.

Oxidative Degradation

It has been shown that oxidation is the primary mechanism of weight loss for most polymers (7). Usually, oxidation is a diffusion limited, or first order, process. This often results in an outer oxidized layer of the material having different material properties than the inner unoxidized region. The oxidized region is typically characterized by embrittlement and an increase in density (4). This can lead to the development of cracks which provide additional pathways for oxygen diffusion and oxidation into deeper regions (11). In general, the degradation of a polymer matrix composite depends on the rate of oxygen diffusion as well as the oxidation reaction rate itself.

In light of this fact, Colin et al (12) developed a kinetic model to predict the thickness of the oxidized layer of F655-2 type poly(bismaleimide). Three sets of experiments were executed. The first was to determine solubility and diffusivity of O_2 in the polymer. Solubility determines the concentration of oxygen in the polymer at its edges exposed to the atmosphere. Diffusivity is used in determining the rate of diffusion of oxygen into deeper regions of the polymer. The second set of experiments determined the critical sample thickness, below which the sample oxidized uniformly, or independent of diffusion effects. Lastly, isothermal gravimetry was performed on samples below the critical thickness to determine kinetics parameters for various temperatures and oxygen pressures.

The model suggested by Colin et al is based on a differential equation in which O_2 diffusion and consumption rate are linked:

$$\frac{\partial C}{\partial t} = D\frac{\partial^2 C}{\partial x^2} - r(C) \tag{8}$$

where C is the O_2 concentration in the polymer, D is an O_2 diffusion coefficient for the polymer, x is the measure of depth into the sample, and r(C) is the rate of O_2 chemical consumption. The steady state rate of O_2 chemical consumption is represented by the following equation, the derivation of which is provided in the *Theory* section.

$$r(C) = 2r_0 \frac{\beta C}{1+\beta C}\left[1 - \frac{\beta C}{2(1+\beta C)}\right] \tag{9}$$

In this equation β is a parameter that nondimensionalizes the concentration field and r_0 is the saturation reaction rate, or the reaction rate in O_2 excess. Using these two equations, the oxygen concentration distributions C(x) can be determined throughout the sample (12). The concentration distribution is important because it governs the rate of oxidation for every depth within the polymer.

Using a closed loop mechanistic scheme explained in the *Theory* section, Colin et al related the rate of O_2 consumption to weight loss of the polymer. The scheme used predicts the autocatalytic effect of oxygen on polymer weight loss that was also observed by Rodriguez-Arnold et al. The thickness profiles of oxidation rate, weight loss, and oxidation products concentration could then be predicted with this model. Colin et al found that experimental results were in agreement with the model's determination of oxidation layer thickness. Weight loss curves for the bismaleimide displayed an initial period of weight gain followed by a nearly constant rate of weight loss. However, the

model proposed here only predicts the steady state weight loss portion of gravimetric curves.

In a later study, Colin et al (13) proposed a model to predict the weight loss and thickness of the oxidized layer of an aromatic amine crosslinked epoxy (ACE) network when aged in air. As in their study of poly(bismaleimide), the model was based on a differential equation which couples diffusion and chemical consumption rate. Additionally, the same closed loop general oxidation scheme was applied.

The resulting predictions for weight loss in ACE were not in as good agreement with the data as was the case with bismaleimides. This was attributed to the depletion of substrates in the polymer network, meaning the sites within the polymer's molecular structure involved in oxidation were being exhausted. Colin et al proposed that substrate depletion is much more rapid in ACE than in polyimides, resulting in rates of weight loss in ACE decreasing as the polymer degraded.

The model was later improved to take into account the decreasing abstractable hydrogen substrate availability for both amine crosslinked epoxy (ACE) and bismaleimide (BMI) (7). This model fit gravimetric curves well up to 12% mass loss for BMI, as opposed to 8% mass loss (BMI) with previous models (7).

In this study, isothermal aging was performed in oxygen excess on thin samples so the effects of oxygen diffusion could be ignored (zero-order kinetic regime). A new parameter γ was introduced which allows differential equations to be developed that account for the decreasing rate of weight loss behavior displayed by gravimetric curves as the substrate availability decreases.

It was suggested that the main difference between gravimetric curves for ACE and BMI, the existence of initial weight gain in BMI, can be attributed to higher hydroperoxide stability in BMI (7). As explained later in the *Theory* section, oxidative weight loss is linked to hydroperoxide decomposition. Higher hydroperoxide stability is therefore correlated with lower weight loss. It was also noted that the initial weight gain period is not present in BMI if an adequately high temperature is used. In that case, the steady state weight loss period occurs immediately as in the case of ACE.

The ability of the general oxidation scheme to be applied to different types of polymers is noteworthy. This allows a model to be built that can be applied to a wide range of polymer matrix composites. Even though the gravimetric curves of BMI and ACE look very different, it is apparent that the same generalized process is responsible for their weight loss. Because the model developed by Colin et al is founded on the fundamental reactions of oxidation, it is better suited to describe gravimetric data than the more empirical models discussed in the *Simple Kinetic Models* section.

The mechanistic scheme that was used with success on BMI and ACE was later applied to PMR-15 by Pochiraju et al (11). In their model, the problem of the decreasing availability of polymer to be oxidized was addressed with a new parameter φ_{ox}. This parameter represents the weight of the completely oxidized material divided by the weight of the unoxidized original material. Where the parameter γ is used by Colin et al to continuously account for decreasing availability of oxidation sites in the polymer, φ_{ox} uses a Boolean approach. The rate of oxidation is considered constant until the weight loss state φ is equal to φ_{ox} at which time the rate of oxidation is turned off.

$$R(C)=\begin{cases} R_0 \dfrac{2\beta C}{1+\beta C}\left[1-\dfrac{\beta C}{2(1+\beta C)}\right]: & \varphi<\varphi_{ox} \\ 0: & \varphi=\varphi_{ox} \end{cases} \tag{10}$$

When oxidation reaction rate R(C) is zero at a particular depth in the polymer, O_2 diffusion deeper into the sample dominates, and the oxidation layer thickness increases.

The need for the parameter φ_{ox} in modeling oxidation layer growth results from the existence of an outer layer of oxidized material that exhibits a low rate of oxidation relative to the actively oxidizing inner layer. Pochiraju and Tandon observed that cross-sections of aged PMR-15 exhibit three distict regions: an inner unoxidized region ($\varphi=0$), an outer oxidized region $\varphi=\varphi_{ox}$, and a thin region in between which represents the actively oxidizing region ($\varphi<\varphi_{ox}$) (11). Pochiraju et al also observed that the diffusivity of the outer oxidized polymer layer is not the same as that of the unoxidized polymer, and that it is the diffusivity of the oxidized polymer that controls the growth of the oxidized layer.

In their model, weight loss was correlated to rate of O_2 consumption in the following manner:

$$\frac{d\varphi}{dt}=-\alpha R(C) \tag{11}$$

It was decided that the parameter α is time dependent because more than one mechanism maybe responsible for weight loss and different mechanisms may become significant at different times. This, of course, is particularly true if the material first undergoes a weight gain, as is the case in bismaleimides.

Bismaleimides

As mentioned before, aromatic polyimides are widely utilized in aeronautical applications for their high thermal stability. One such polyimide, PMR-15, is often used for high temperature polymer matrix composites for temperature use in the range of 232^0C because of its excellent elevated temperature properties (14). However, PMR-15 contains 4,4'-methylenedianiline (MDA) which is a kidney and liver toxin, and a suspected carcinogen (15). Processing difficulties and micro-cracking are also problems of PMR-15 which have increased interest in bismaleimide (BMI) resins which can be used at a lower cost (16) . Furthermore, BMI resins facilitate the use the resin transfer molding (RTM) process. Resin transfer molding involves impregnating a fiber preform with low viscosity liquid resin which is then cured. Conversely, PMR-15 parts are generally made with more difficulty by hot-pressing layers of prepreg together at high temperature.

BMIs are a class of aromatic polyimides whose monomer building blocks are synthesized from aromatic diamines and maleic anhydride (2). They generally have a service temperature above those of epoxies, but lower than the service temperature of PMR-15. A commonly used BMI component is 4,4-bismaleimidodiphenylmethane (BMDPM). As seen in Figure 1, BMDPM has two maleimide groups each attached to the fourth carbon of an aromatic ring. According to Torrecillas et al, BMDPM can form a cross-linked network via the double bonds on the maleimide groups changing to single

bonds, allowing those carbons to form single bonds to analogous carbons on other monomers (17).

Aromatic rings, common in thermostable polymers, contain six carbons that have alternating single and double bonds between them. Although the locations of the double bonds are pictured in the aromatic rings of BMDPM, it is more realistic to visualize the electrons of those double bonds as being delocalized over the entire ring. This sharing of electrons is responsible for the stability of the aromatic rings. That being said, the least thermostable locations of a network formed from BMDPM are between the aromatic rings (17).

BMIs are addition type polymers, meaning they polymerize without the elimination of by-products. Like other thermosetting polymers, the polymerization process eventually produces a cross-linked, infinite three-dimensional structure of covalent bonds (6).

5250-4 Literature Review

5250-4 is a BMI resin introduced by Cytec Engineered Materials nearly 20 years ago. Its relatively high service temperature and ease of processing have made 5250-4 RTM a common aerospace resin that is currently being used on the F-22 and the Joint Strike Fighter (14). A study by Biney et al has also shown IM7/5250-4 to be possibly useful as a material for cryogenic propellent tanks used on reusable space launch vehicles (18). Figure 1 contains diagrams of the three main components of 5250-4 RTM (19).

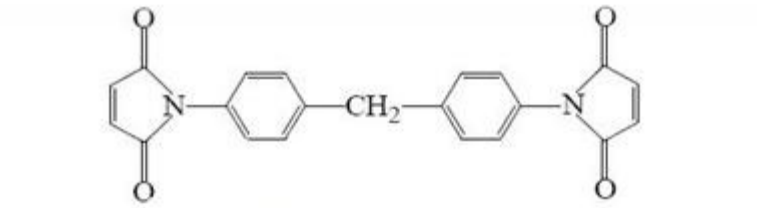

4,4' -Bismaleimidodiphenylmethane

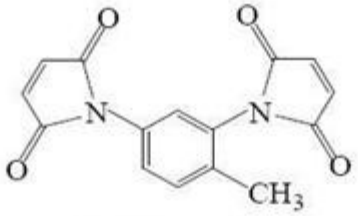

BMI- 1,3-tolyl

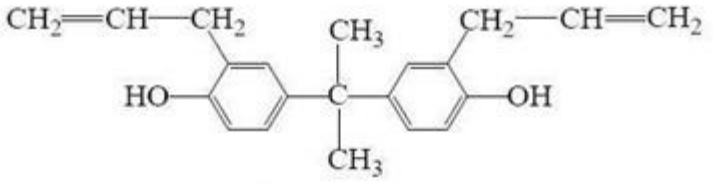

o,o'-Diallylbisphenol A

Figure 1: Components of 5250-4 RTM (19)

It contains the commonly used BMDPM monomer and another bismaleimide, BMI 1,3-tolyl. Like BMDPM, BMI 1,3-tolyl has two maleimide groups which can be seen on the first and third carbon of the central aromatic ring. Additionally, a methyl group (CH_3) is located on the sixth carbon. The o,o'-diallylbisphenol A (BPA) monomer in Figure 1 is not a bismaleimide, but it is often used in BMI polymers to make otherwise brittle BMIs more processable (20).

Bongiovanni et al carried out aging experiments on composites made of epoxy systems, as well as the 5250-4 resin system. They showed that the open-hole compression (OHC) strength of the 5250-4 resin composite remained above 207 MPa for

a 177^{0}C wet environment. This is a typical metric to define the service temperature for a composite (14). Additionally it was determined that 5250-4 has a damage tolerance equal to that of medium toughness epoxies, which have become the industry standard for evaluation.

Bongiovanni et al also performed weight loss experiments in air at 232^{0}C on the 5250-4 composites. It was determined that the outer most ply was oxidizing, and weight loss occurred as a result of carbon dioxide, water, and other gasses escaping (14). The glass transition temperature (T_g) was also discovered to increase by approximately 30^{0}C after aging for 2000 hours in a 232^{0}C air environment. The increase in glass transition temperature is generally caused by additional cross-linking in the polymer network.

Boyd et al aged composites of 5250-4 and various fibers in air at 177^{0}C, 205^{0}C, and 232^{0}C for up to one year. The weight and various mechanical properties of the composites were measured before and after aging. After one year of aging a 5250-4 composite panel in a 177^{0}C air circulating oven, the panel lost only 0.8% of its initial weight (16). Boyd also investigated the effect of different fibers on the weight loss of the composites. Three different fiber types, two with intermediate modulus and one standard modulus fibers, were evaluated. It was determined that weight loss was independent of fiber type, at least for the fibers considered (16) .

After aging in air for one year at 177^{0}C, the 5250-4 composite panels had a compression after impact (CAI) strength approximately equal to that of an un-aged panel. Conversely, the panels aged at 205^{0}C exhibited a 40% loss of CAI strength (16). Aging in a nitrogen environment at this temperature showed that this loss of strength was not the

result of an oxidative process. Weight loss, however, was the result of an oxidative process.

BMIs tend to absorb moisture from the environment due to an assortment of polarized groups in their molecular structure (21). This can lead to plasticization and accelerated thermal degradation when combined with high temperatures. Moreover, increased temperature accelerates moisture absorption of BMIs (22). Biney et al conducted aging experiments on IM7/5250-4 composites in both air and saturated steam to investigate hydrolytic and thermal aging of the composite (21). Thermal aging was carried out at 200^0C for 96 hours, 192 hours, and 384 hours, while hydrolytic aging was carried out for 48 hours, 96 hours, 144 hours, and 192 hours at the same temperature. After each aging period, the aged composite underwent a short beam shear test, dynamic mechanical analysis, dynamic thermo-gravimetric analysis, and observation with scanning electronic microscopy. It was found that resin loss and mechanical properties were indeed exacerbated by the presence of moisture. According to a study by Li-Rong Bao et al, the degradation of 5250-4 in a wet environment results from hydrolysis of the polyimide rings (22), some of which can be seen in Figure 1.

As mentioned earlier in this section, φ_{ox} is a parameter used in the Pochiraju and Tandon model of oxidative layer growth to indicate the conversion state at which the polymer no longer appreciably oxidizes. This parameter has been used in the successful modeling of PMR-15 oxidative layer growth, which displays three distinct oxidation regions (11). 5250-4, on the other hand, does not display three distinct regions of oxidation. One method of tracking oxidative layer growth is to identify the elastic modulus of the material as a function of depth using a nanoindentation technique. Recent

AFRL studies indicate that the elastic modulus of 5250-4 increases continuously from the inner region to the free edge of the sample (23). With a three region model, one would expect to find a region near the free surface where modulus does not change. This indicates that 5250-4 may be better represented by two regions: an un-oxidized center and an actively oxidizing region that continues to degrade. This suggests the use of the parameter φ_{ox} may be inappropriate for representing oxidation of 5250-4 bismaleimide resin.

Objective of Thesis

The Air Force Research Laboratory is interested in developing a predictive model for the lifetime performance of high temperature matrix composites. Describing the degradation of a polymer matrix composite is complicated by heterogeneous nature of the process. Thermal degradation, thermo-oxidative degradation, and hygrothermal degradation can all occur simultaneously. Oxidation and hygrothermal degradation, furthermore, are diffusion controlled, and therefore depend on the diffusivity and geometry of the PMC. Additionally, the matrix material and the fiber material will degrade differently. Phenomena at the matrix fiber interface can further complicate lifetime performance prediction by introducing fiber-matrix residual stresses (4) or providing new pathways for oxygen diffusion (11). Multiscale modeling levels are thus necessary to effectively predict lifetime performance of polymer matrix composites (4).

According to Schoeppner et al, there are five main levels of multiscale modeling necessary for lifetime performance prediction. The lowest level of the multiscale model is the chemical degradation of the matrix and fibers materials by themselves, which

depend on their respective chemical structures. Moving up in the multiscale hierarchy, the constituents of the composite must be modeled, which takes into effect the geometry and diffusivity characteristics of the constituents. Next, the effects on degradation of the interface between matrix and fiber must be incorporated into the model. After the matrix, fiber, and interfacial effects are understood, it is necessary to evaluate the effect of micromechanics on the degradation of the composite. Lastly, ply-level modeling must be done for accurate lifetime prediction of polymer matrix composite parts.

This thesis fits into the multiscale modeling process at the lowest level: modeling thermo-oxidative degradation of a high temperature polymer. Similar to previous work on PMR-15 by Grant Robinson (24), in this thesis isothermal weight loss measurements were recorded to evaluate kinetics parameters for 5250-4. The following test matrix was provided by Dr. Greg Schoeppner of the Air Force Research Laboratories Materials and Manufacturing Directorate at Wright-Patterson Air Force Base.

Table 1: Test Conditions for 5250-4 Powder aging of 250 hours

Temperature (^{0}C)	Argon	Air	Oxygen
163	X	X	X
177	X	X	X
190	X	X	X

The 5250-4 resin was made into a powder to eliminate the limiting effect of oxygen diffusion into a solid sample. Each test was run for at least 250 hours. Argon was used as an inert aging environment to measure non-oxidative weight loss, and two different partial pressures of oxygen were tested by utilizing pure oxygen and air.

Normalized weight, equal to the weight of the material (W) divided by the original weight of the material (W_0), was used in this thesis for easy comparison with research of the degradation of other polymer systems. Weight loss was therefore defined as $L=1-W/W_0$.

The parameters of the model used by Pochiraju and Tandon, as described on page 14, were evaluated for 5250-4. These parameters include the normalized concentration parameter (β), the weight loss to reaction rate correlation constant (α), and the saturated reaction rate (r_0). The oxidation rate constants described in the closed loop mechanistic scheme in the following *Theory* section, were also evaluated to determine if oxidative degradation of 5250-4 could be represented by the model proposed by Colin et al.

The concept of equivalent property time was also applied to determine if it is a legitimate means of interpolating weight loss curves for 5250-4 at temperatures within the bounds of the test matrix in Table 1. The derivation of equivalent property time is also included in the *Theory* section to follow.

II. Theory

This section describes in detail the equations from the literature which were applied to 5250-4 weight loss data in this thesis.

Closed Loop Mechanistic Scheme for Polymer Oxidation

The primary means of thermal degradation of polymers are radical chain processes (6). Radicals are atoms or molecules that contain an unpaired electron which makes them very reactive. Once formed in a polymer, they start a chain reaction which results in the breaking of polymer bonds and degradation of the material.

A considerable amount of literature is dedicated to using a mechanistic scheme in which radical production is exclusively the result of hydroperoxide decomposition to model thermal oxidation for high temperature polymers (7, 12, 13, 25). This means that generation of radicals from polymer thermolysis, where polymer bonds dissociate solely with added heat, is ignored. It is safe to assume that radical production by thermolysis is negligible under 250^0C for thermostable polymers (26). This assumption is justified because in thermostable polymers, most polymer bonds have a dissociation energy that is much larger than that of hydroperoxides (12).

According to Colin et al (7), the general oxidation scheme is represented by the six steps shown in Table 2.

Table 2: Generalized Steps of Polymer Oxidation (7)

Step		General Reaction	Rate Constants
(I)	Initiation	$POOH+\gamma PH \rightarrow 2P^{\circ}+H_2O+\upsilon V$	(k1)
(II)	Propagation	$P^{\circ}+O_2 \rightarrow PO_2^{\circ}$	(k2)
(III)	Propagation	$PO_2^{\circ}+PH \rightarrow POOH+P^{\circ}$	(k3)
(IV)	Termination	$P^{\circ}+P^{\circ} \rightarrow$ inactive products	(k4)
(V)	Termination	$P^{\circ}+PO_2^{\circ} \rightarrow$ inactive products	(k5)
(VI)	Termination	$PO_2^{\circ}+PO_2^{\circ} \rightarrow$ inactive products$+O_2$	(k6)

Here, POOH represents a general hyroperoxide. P^{o} represents an alkyl radical, which is a radical produced from an alkyl substituent group. An alkyl group is a side group of carbon and hydrogen on the polymer resembling an alkane (C_nH_{2n+2}) less one hydrogen. PO_2^{o} represents peroxyl radicals which are formed with the addition of oxygen to alkyl radicals. PH represents what Colin et al call substrate, or the sites in the polymer's molecular structure of hydrogens which can be removed to form hydroperoxides as in the propagation step (III) or water as in step (I).

The initiation step in this scheme represents the decomposition of hydroperoxides, POOH. Initially, there are few hydroperoxide sites in the polymer. However, after radicals produced in the first step react with oxygen, they are capable of abstracting hydrogen atoms and producing more hydroperoxides. Such a scheme is often called a closed loop mechanistic scheme because the reaction produces its own initiator as a product, as shown by the hydroperoxide generation in step (III). This can explain the autocatalytic effects demonstrated by some polymers in oxidative environments.

There are two possible forms of the hydroperoxide decomposition of the initiation step (25). The form of step (I) above represents unimolecular POOH decomposition. Bimolecular decomposition may also be taking place during initiation, taking the following form (25):

$$2POOH+\gamma PH \rightarrow P^{\circ}+PO_2{}^{\circ}+H_2O+\upsilon V \quad (12)$$

Bimolecular decomposition can occur if hydroperoxides are hydrogen bonded together, whereas unimolecular decomposition takes place when hydroperoxides are separate (25). According to Colin et al (26), unimolecular decomposition is predominant at temperatures above 120^0C. At temperatures of this magnitude, the hydrogen bonds necessary to facilitate bimolecular decomposition are broken before the hydroperoxides decompose (25).

In the initiation step, volatiles are formed with V representing an average volatile molecule with yield υ. As mentioned earlier, the γ term accounts for the availability of abstractable hydrogens in the initiation step (26). This term allows for the model to represent the reduced rate of weight loss displayed by gravimetric curves after high weight loss when the availability of substrate PH diminishes. Finally, the rate constants for each step of the scheme (k_1, k_2,…,k_6) are functions of temperature by means of an Arrhenius relationship (6).

Differential equations can be constructed from the six general reactions to describe the time rate of change of the radicals (P^0, $PO_2{}^0$), hydroperoxides (POOH), and substrate (PH) concentrations. This is done by considering which steps a particular species results from, and at what rate the step propagates.

For example, to find the time rate of change of peroxyl radical concentration it is noted that $PO_2{}^0$ is produced in step (II) Propagation by combining P^0 and O_2. The

production of oxide radicals in this step occurs at a rate equal to the product of the reactants' concentrations multiplied by the step's rate constant:

$$\text{Rate of Production of } PO_2{}^0 = k_2[O_2][P^0] = k_2[C][P^0] \tag{13}$$

where [C] represents the concentration of O_2. Similarly, the steps where $PO_2{}^0$ is consumed are considered (Termination steps V and VI).

$$\text{Rate of } PO_2{}^0 \text{ depletion} = k_5[P^0][PO_2{}^0] + k_6[PO_2{}^0]^2 \tag{14}$$

Subtracting the rate of depletion from the rate of production gives the time rate of change of $PO_2{}^0$:

$$\frac{d[PO_2{}^\circ]}{dt} = k_2C[P^\circ] - k_3[PH][PO_2{}^\circ] - k_5[P^\circ][PO_2{}^\circ] - 2k_6[PO_2{}^\circ]^2 \tag{15}$$

The time rates of change of the other species are similarly determined (26):

$$\frac{d[P^\circ]}{dt} = 2k_1[POOH] - k_2C[P^\circ] + k_3[PH][PO_2{}^\circ] - 2k_4[P^\circ]^2 - k_5[P^\circ][PO_2{}^\circ] \tag{16}$$

$$\frac{d[PO_2{}^\circ]}{dt} = k_2C[P^\circ] - k_3[PH][PO_2{}^\circ] - k_5[P^\circ][PO_2{}^\circ] - 2k_6[PO_2{}^\circ]^2 \tag{17}$$

$$\frac{d[POOH]}{dt} = -k_1[POOH] + k_3[PH][PO_2^\circ] \tag{18}$$

$$\frac{d[PH]}{dt} = -\gamma k_1[POOH] - k_3[PH][PO_2^\circ] \tag{19}$$

The rate of change of polymer weight can then be determined by considering the steps where water and volatiles are released (I Initiation) and the rate of oxygen incorporation into the polymer:

$$\frac{1}{m_0}\frac{dm}{dt} = \frac{32}{\rho_0}(R(C)) - \frac{18}{\rho_0}k_1[POOH] - \frac{\nu M_v}{\rho_0}k_1[POOH] \tag{20}$$

In this equation, the first term of the polynomial represents the oxygen incorporation into the material with R(C) representing the O_2 consumption rate represented as

$$R(C) = -\frac{d[O_2]}{dt} = k_2 C[P^\circ] - k_6[PO_2^\circ]^2 \tag{21}$$

The next two terms of the polynomial represent weight change as a result of H_2O and volatile evolution respectively, both of which are related to the availability of hydroperoxides [POOH] and the rate constant k_1 of initiation (I). The coefficients of each of the terms of the weight loss rate represent the weights of oxygen (molecular

weight 32), water (molecular weight 18), and volatiles. The molecular weight of the volatiles released is represented by the parameter νM_v, the effective molecular weight and yield of an average volatile. The molecular weights have units [g mol^{-1}], and the concentrations have units of [mol l^{-1}] so each term must be divided by the original density of the polymer [g l^{-1}] to make the rate of weight change unitless.

The set of ordinary differential equations (equations 15, 16, 17, 18, 19, and 20) can be solved numerically as demonstrated by Colin et al (26) to predict the weight loss of a polymer. It is assumed that the initial concentrations of radicals $[P^o]_0$ and $[PO_2^o]_0$ are zero at time t=0. The initial substrate concentration $[PH]_0$ can be determined with knowledge of the chemical structure of the polymer, usually being equal to the concentration of certain hydrocarbon substituents in the original polymer (7). The initial concentration of hydroperoxides $[POOH]_0$ is assumed to be very small at time zero. However, assuming radicals are only produced from hydroperoxide decomposition, $[POOH]_0$ must be non-zero. Otherwise the reaction would not take place as shown in the above differential equations. The initial POOH concentration will generally depend on how the polymer was manufactured and stored. This appears to add another unknown to a large set of parameters. However, according to Audouin et al (25), the induction time for the reaction under unimolecular decomposition is relatively insensitive to initial POOH concentrations. The rate constants, however, are harder to determine.

Some rate constants can be assumed from the chemical composition of the polymer. The rate constant k_3 for example, which determines the rate at which peroxyl radicals react with substrate to produce hydroperoxides, has been determined for a number of common CH substituents (7). The rate constant k_2, which determines the rate

at which oxygen reacts with P^0 radicals, can also be determined from previously established rate constants for a number of compounds (26). The rest of the parameters must be determined by selecting the set of parameters which result in a model that best represents experimental data (7).

Steady State Oxidation Rate Utilized in the AFRL Weight Loss Model

The system of differential equations (equations 15, 16, 17, 18, 19, and 20) must be solved numerically to determine the oxidative weight loss of a polymer. However, a closed form solution can be reached if only the steady-state portion of the reaction is considered. The steady state oxidation R(C), as used by Pochiraju and Tandon in their study of PMR-15 (11), is derived by making these simplifying assumptions. The derivation, according to Colin et al, is included below (12).

In the steady-state condition, the time rate of change of radicals is assumed to be zero so that

$$\frac{d[P^\circ]}{dt} = 0 = 2k_1[POOH] - k_2C[P^\circ] + k_3[PH][PO_2^\circ] - 2k_4[P^\circ]^2 - k_5[P^\circ][PO_2^\circ] \qquad (22)$$

and

$$\frac{d[PO_2^\circ]}{dt} = 0 = k_2C[P^\circ] - k_3[PH][PO_2^\circ] - k_5[P^\circ][PO_2^\circ] - 2k_6[PO_2^\circ]^2 \qquad (23)$$

Adding equation 22 and equation 23 results in the following

$$2k_1[POOH]-2k_4[P]^2-2k_5[P][PO_2]-2k_6[PO_2]^2=0 \quad (24)$$

The concentration of hydroperoxides is also assumed to be constant in the steady-state, as shown as

$$\frac{d[POOH]}{dt}=0=-k_1[POOH]+k_3[PH][PO_2^\circ] \quad (25)$$

Solving for $k_1[POOH]$ and substituting into equation 24 results in the following relationship

$$2k_3[PH][PO_2^\circ]-2k_4[P^\circ]^2-2k_5[P^\circ][PO_2^\circ]-2k_6[PO_2^\circ]^2=0 \quad (26)$$

which can then be solved for $[P^0]$.

$$[P^\circ]=\frac{-k_5[PO_2^\circ]\pm\sqrt{k_5^2[PO_2]^2-4k_4(k_6[PO_2^\circ]^2-k_3[PO_2][PH]}}{2k_4} \quad (27)$$

Dropping the meaningless negative radical concentration, and rearranging yields

$$[P^{\circ}]=\frac{-k_5[PO_2^{\circ}]+k_5[PO_2^{\circ}]\sqrt{1-\frac{4k_4k_6}{k_5^{\,2}}+\frac{4k_4k_3[PH]}{k_5^{\,2}[PO_2^{\circ}]}}}{2k_4} \tag{28}$$

$$[P^{\circ}]=\frac{k_5[PO_2^{\circ}]}{2k_4}\left\{-1+\sqrt{1+\frac{4k_4k_6}{k_5^{\,2}}\left(-1+\frac{k_3[PH]}{k_6[PO_2^{\circ}]}\right)}\right\} \tag{29}$$

In oxygen excess, the concentration of $[P^0]$ will go to zero when all of the $[P^0]$ radicals will react to become $[PO_2{}^0]$. This will correspond to the time when $[PO_2{}^0]$ is at its maximum concentration. As seen in equation 29, $[P^0]$ will go to zero when

$$\left(-1+\frac{k_3[PH]}{k_6[PO_2^{\circ}]}\right)=0 \tag{30}$$

$$[PO_2^{\circ}]_0=\frac{k_3[PH]}{k_6} \tag{31}$$

where $[PO_2{}^0]_0$ is the maximum concentration of peroxyl radicals. The equation can now be simplified to

$$[P^{\circ}]=\frac{k_5[PO_2^{\circ}]}{2k_4}\left\{-1+\sqrt{1+\psi\left(\frac{[PO_2^{\circ}]_0}{[PO_2^{\circ}]}-1\right)}\right\} \tag{32}$$

where

$$\psi=\frac{4k_4k_6}{k_5^{\,2}}\ll 1 \tag{33}$$

Considering the case where $[PO_2^0]$ is near its maximum value, Colin et al make the following approximation (27)

$$\left\{-1+\sqrt{1+\psi\left(\frac{[PO_2^\circ]_0}{[PO_2^\circ]}-1\right)}\right\}\approx\frac{\psi}{2}\left(\frac{[PO_2^\circ]_0}{[PO_2^\circ]}-1\right) \tag{34}$$

Substituting 34 into equation 32 results in

$$[P^\circ]=\frac{k_6}{k_5}([PO_2^\circ]_0-[PO_2^\circ]) \tag{35}$$

which can be substituted into equation 23 to produce

$$0=k_2C\frac{k_6}{k_5}\left([PO_2^\circ]_0-[PO_2^\circ]\right)-k_3[PH][PO_2^\circ]-k_6([PO_2^\circ]_0-[PO_2^\circ])[PO_2^\circ]-2k_6[PO_2^\circ]^2 \tag{36}$$

which can be solved for the concentration of peroxyl radicals:

$$[PO_2^\circ]=[PO_2^\circ]_0\frac{\beta C}{1+\beta C} \tag{37}$$

where

$$\beta=\frac{k_2k_6}{2k_5k_3[PH]} \tag{38}$$

By substituting equation 37 into equation 35 one obtains

$$[P^{\circ}]=\frac{k_6}{k_5}\left([PO_2^{\circ}]_0-[PO_2^{\circ}]_0\frac{\beta C}{1+\beta C}\right) \tag{39}$$

or

$$[P^{\circ}]=\frac{k_6[PO_2^{\circ}]_0}{k_5}\left(1-\frac{\beta C}{1+\beta C}\right) \tag{40}$$

$$[P^{\circ}]=\frac{k_6[PO_2^{\circ}]_0}{k_5}\left(\frac{1}{1+\beta C}\right) \tag{41}$$

Recalling the definition of R(C) in equation 21, equations 41 and 37 can be substituted to produce

$$R(C)=k_2C\frac{k_6[PO_2^{\circ}]_0}{k_5}\left(\frac{1}{1+\beta C}\right)-k_6[PO_2^{\circ}]_0^{\,2}\left(\frac{\beta C}{1+\beta C}\right)^2 \tag{42}$$

$$R(C)=\frac{2k_3^{\,2}[PH]^2}{k_6}\left(\frac{\beta C}{1+\beta C}\right)-k_6\left(\frac{k_3[PH]}{k_6}\right)^2\left(\frac{\beta C}{1+\beta C}\right)^2 \tag{43}$$

$$R(C)=2r_0\left(\frac{\beta C}{1+\beta C}\right)\left[1-\frac{\beta C}{2(1+\beta C)}\right] \tag{44}$$

where the saturation reaction rate r_0 is defined as

$$r_0=\frac{k_3^{\,2}[PH]^2}{k_6} \tag{45}$$

Equation 44 represents the steady-state rate of reaction with oxygen for which the parameters β, α, and r_0 must be determined for the AFRL modeling efforts.

Equivalent Property Time

Equivalent property time, as applied to polymer aging by Seferis (8), is derived in this section. In his application, conversion (a) was defined as the weight loss of the polymer normalized by the total weight loss at the conclusion of aging.

$$a=\frac{M_0-M}{M_0-M_f} \tag{46}$$

The familiar rate of degradation is used again:

$$\frac{da}{dt}=kf(a) \tag{47}$$

Where f(a), the kinetic model, is a function of conversion. k is a temperature dependent rate constant given by the Arrhenius relation

$$k=A\exp\left(\frac{-E}{RT}\right) \tag{48}$$

where E is activation energy, R is the gas constant, and T is temperature. Various forms of f(a) can be used to characterize different types of polymer weight loss as demonstrated by Rodriguez-Arnold et al (10) and by Regnier and Guibe (1). However, the method of equivalent property time conveniently removes the need for finding such a function of conversion.

By separation of variables and integration at a constant temperature of equation 47, the following expression is obtained:

$$G(a)=\int_{a1}^{a2}\frac{da}{f(a)}=\int_{0}^{t}kdt \tag{49}$$

$$G(a)=kt \tag{50}$$

Because G(a) is only a function of conversion, and it is assumed to be independent of temperature, it can be cancelled by dividing equation 50 of one temperature T_1 by the same equation at a second temperature T_2.

$$1=\frac{k_{T_1}t_{T_1}}{k_{T_2}t_{T_2}} \tag{51}$$

which leads to

$$t_2=t_1\frac{A\exp\left(\frac{-E}{RT_1}\right)}{A\exp\left(\frac{-E}{RT_2}\right)} \tag{52}$$

Assuming A, E, and R are independent of temperature in the range of temperatures considered, this expression can be simplified:

$$t_2=t_1e^{\left[\frac{E}{R}\left(\frac{1}{T_2}-\frac{1}{T_1}\right)\right]} \tag{53}$$

With this equation, Seferis demonstrated that the time t_1 at which a particular conversion is reached at a temperature T_1, can be converted to the equivalent property time, t_2, at

which the same conversion will be reached at temperature T_2. The activation energy divided by the gas constant, E/R, can be determined by measuring the change of ln(t) divided by the change in 1/T for equal conversions at two isothermal temperatures (8). This concept was applied to 5250-4 in this Thesis to determine if it is a valid means of producing gravimetric curves within the temperature range considered.

III. Materials, Equipment, and Experimental Procedure

This section of the Thesis describes the processing of the material for the experiments, the equipment used, and the procedure that was applied. The methodology has been previously established and used with success by Grant Robinson (24).

Material Processing

Cure and Post Cure

The 5250-4 resin was obtained from Cytec Engineered Materials Technical Services. The resin was stored in a freezer at the recommended -18^{0}C prior to processing. Processing and cure of the 5250-4 was already completed for previous research by 2nd Lt John G. Balaconis (28). This section outlines his procedure for the processing and cure of the 5250-4.

The first step was to place the frozen resin into an aluminum pan, which was then set in a vacuum oven at 100^{0}C for one hour to remove any residual water from the resin. After 60 minutes, the now liquid resin was placed into a conventional oven at 131^{0}C. The resin was held at this temperature for 10 minutes, after which the resin was poured into a glass mold. Once in the mold, the resin was placed back into the oven, and held at 131^{0}C for another 30 minutes to allow air bubbles to escape from the mold. After the air had escaped, the temperature was slowly increased to 191^{0}C at a rate of 1^{0}C/min. The 5250-4 was cured at 191^{0}C for 6 hours, after which it was removed from the glass mold and post-cured in a 227^{0}C oven for another 6 hours.

Powder Production

For this research, the 5250-4 was then made into a powder with particle diameter of 45-90 μm using the process developed by Susan Mendenhall (29), and later used by ENS Grant Robinson (24) in their research of PMR-15. The 5250-4 was first cut into small pieces, approximately 1 to 5mm in length, with shears so that it could be further crushed into small fragments. The pieces were then repeatedly crushed between two stainless steel plates with a Wabash 30 Ton Press. After this process, the pieces were reduced to a size that could be milled into a powder.

A ball mill with a ceramic crucible and ball was used to grind the resin into a powder. Approximately 0.5 grams of BMI resin was loaded into the ceramic crucible, and milled for one hour. This process was repeated until approximately 8 grams of powder was obtained.

The resulting powder contained a wide range of particle sizes, from very fine to large coarse particles. Small, round, white spheres were also visible in the milled powder. These particles were assumed to be polished pieces of ceramic which chipped off of the crucible during the ball-milling process. Electro dispersive spectroscopy of both the resin and the white spheres revealed that the white particles contained silicon, zirconium, aluminum, carbon, and oxygen (Figure 2). This confirmed suspicion that contaminants from the crucible and ball were in the BMI powder. Two stainless steel ASTM test sieves, with mesh sizes of 45 and 90 μm, were used to collect only the powder in the 45 to 90 μm range. Contaminants such as the white ceramic material were removed by suspending the 5250-4 in carbon tetrachloride. With a density of 1250 g/l,

the 5250-4 remained suspended in the carbon tetrachloride (1590 g/l) while higher density impurities settled to the bottom.

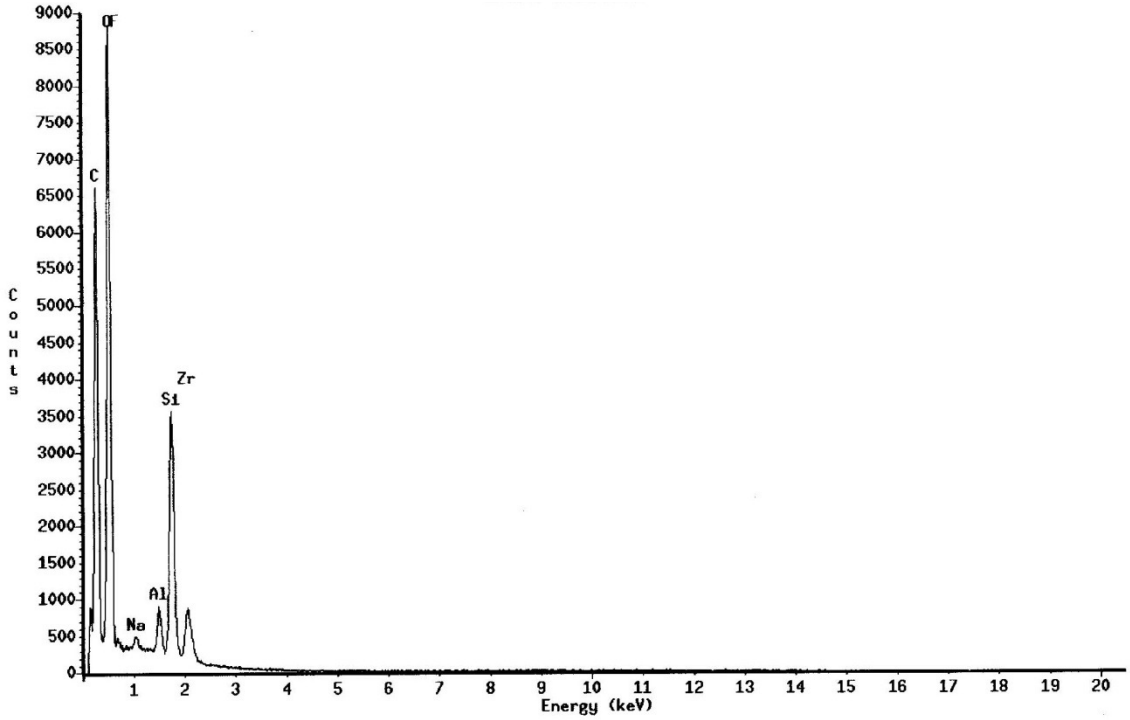

Figure 2: Electro Dispersive Spectroscopy of 5250-4 with contaminants

Fine white particles were observed on the bottom of the CCl_4 beaker. After suspension, the 5250-4 was scooped from the surface of the CCl_4 and placed into a vacuum oven at 49^0C for 20 hours to evaporate the solvent.

Equipment

A Hi-Resolution TGA 2950 Thermo-gravimetric Analyzer, seen in Figure 3, was used to continuously measure the weight of a powdered sample of 5250-4 while aging the material in an isothermal environment of air, oxygen, or argon. The balance of the TGA has a precision of one thousandth of a milligram. The balance is located above the

furnace, so nitrogen was used as a purge gas for the balance to prevent out-gassed volatiles of the polymer from coming into contact with the balance mechanism. A flow rate of 40 ccm of nitrogen was regulated with an Omega Engineering Incorporated FVA-2600A volumetric flow controller for the balance purge gas.

A second flow meter was used to supply 60 ccm of the desired purge gas for the furnace section. This purge gas ensures that the test specimen is exposed to the desired atmosphere by supplying the test gas and purging the furnace of degradation products out-gassed from the specimen. The air, oxygen, and argon purge gas were supplied by high pressure tanks with regulators that reduced the output pressure to approximately 40 psi, an acceptable pressure for the flow meters. Nitrogen was supplied through the house nitrogen system.

Figure 3: TA Instruments Hi-Resolution TGA-2950 Thermo-Gravimetric Analyzer

A sample is loaded into the TGA on a titanium basket, which hangs from the balance on a hook that is suspended in the center of the cylindrical furnace. When in operation, the TGA collects data points for time, temperature, and mass at a specified time interval. The operation of the TGA is controlled by the user with a computer running Thermal Advantage software. This program allows the operator to prescribe a desired temperature versus time profile which the TGA will execute. The operator can also override an experiment by editing the time or temperature of a current segment, or even skip to the next prescribed segment in the temperature profile.

As an experiment progresses, the data is stored by the TGA itself. After completion of the experiment, the data is transferred to a data file which can be imported to Microsoft Excel for analysis.

Experimental Procedure

The titanium basket which held the sample had to be cleaned before each test. This was accomplished by exposing the basket to the flame of a butane torch for several seconds. The clean basket was then loaded into the TGA for the taring process. After the furnace section was sealed, five minutes was allowed to pass to ensure that the purge gas had displaced any laboratory air. Once the wait period was over, the tare function of the TGA set the measured weight of the titanium basket equal to zero milligrams.

The furnace was then lowered, and the basket unloaded. A sample of 10 ± 1 milligrams was placed into the basket on the loading platform as seen in Figure 4. Once the basket, with the sample, was loaded into the TGA with the furnace sealed, five minutes was again allowed to pass.

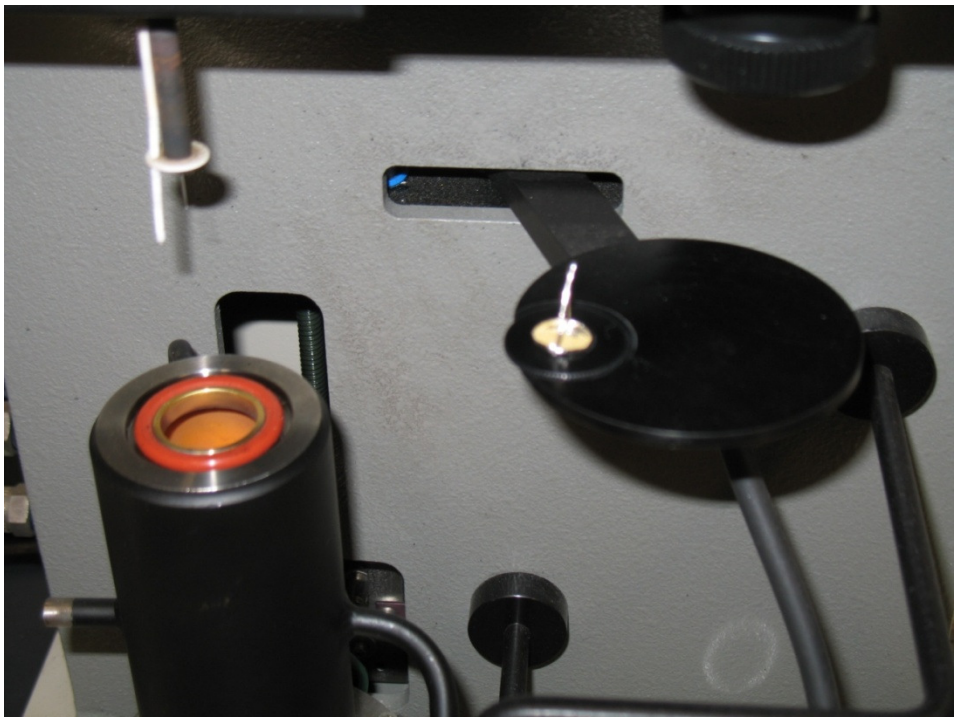

Figure 4: Titanium Basket on loading platform of TGA

During this time, the temperature profile for the test was entered into the PC. Once the TGA was started, it performed all of the heating instructions that were entered prior to the test. Each test started with a 20^0C per minute ramp up to 110^0C. The sample was held at this temperature for 60 minutes to allow any moisture to evaporate. A 100^0C per minute ramp was then used to bring the sample up to the testing temperature in the shortest amount of time possible. Once the test temperature was reached, the TGA maintained that temperature for 250 hours. Throughout the test, the TGA would record the time, temperature, and mass of the sample at intervals of 45 seconds.

The TGA would allow the operator to override the prescribed test profile if needed. This function was used to cut the 110^0C isothermal hold short in cases where the mass was no longer changing. The override function was also used to extend the

isothermal hold time at test temperature in cases where weight loss data beyond 250 hours was desired.

After each test was completed, the TGA saved the data and shut down the furnace. The data was then exported to a data file, and the aged 5250-4 was discarded.

All weights were normalized for easy comparison between results at different temperatures and aging environments. After the moisture evaporation hold period, the weight at the beginning of the isothermal test temperature hold was used as W_0. Normalized weight in all tests, therefore, starts at unity for the isothermal test period.

IV. Results and Analysis

This chapter presents the results of thermo-gravimetric analysis carried out in argon, oxygen, and air.

TGA Results in Argon

Tests in argon were completed first to determine the extent of weight loss in an inert environment. Results of the tests are presented in below in Table 3 and Figure 5.

Table 3: Argon Test Summary

Test Temperature (^{0}C)	**163**	**177**	**190**
110^{0}C Time (min)	120	120	120
Weight loss, 110^{0}C (%)	1.88%	1.92%	2.02%
Isothermal Test Time (hours)	250	250	250
Final Normalized Weight	0.994	0.993	0.991

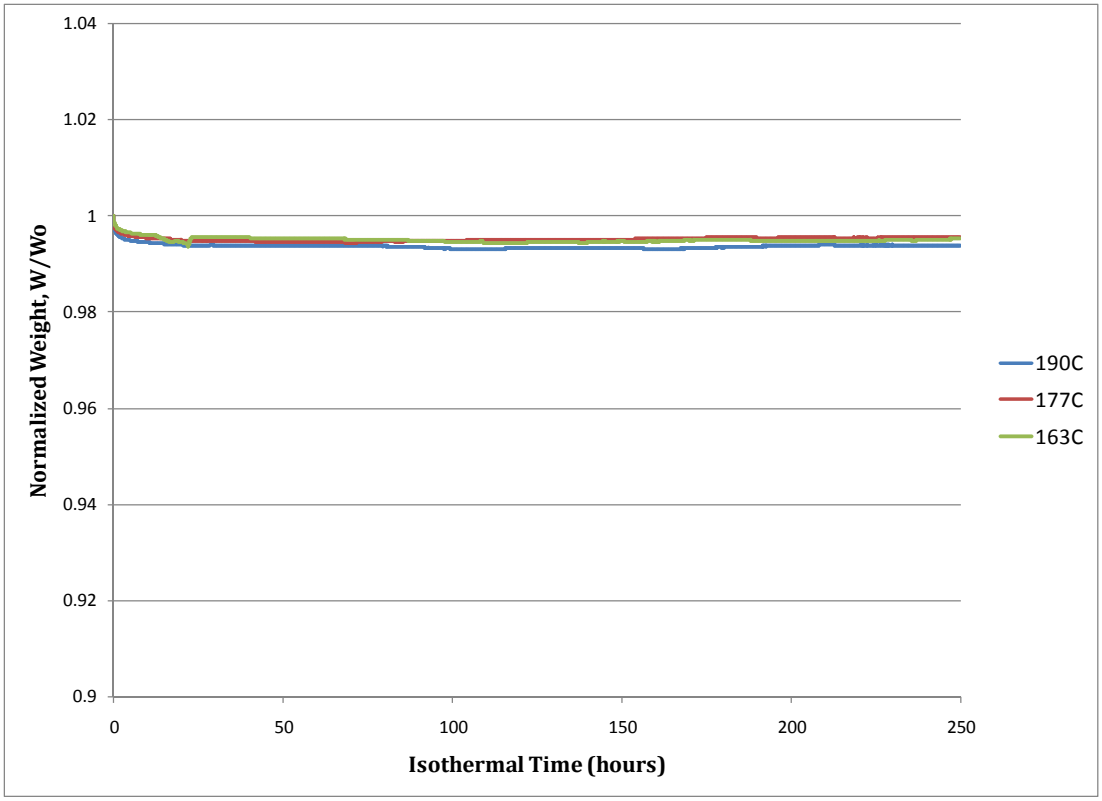

Figure 5: Gravimetric Data of 5250-4 in Argon

As can be seen in Figure 5, after an initial drop in weight early in the isothermal hold, the weight of 5250-4 was relatively constant throughout the remainder of the test. A steep decrease in weight occurs for all temperatures during the first eight minutes, after which the rate of weight loss decreases. A closer look at the initial weight loss is seen in Figure 6. As expected, the 190^{0}C test resulted in the greatest weight loss, followed by the 177^{0}C test, with the 163^{0}C test exhibiting the lowest weight loss. However, it is notable that none of the test temperatures resulted in a weight loss greater than 1% in an argon environment. Additionally, all of this weight loss occurred within the first several hours of testing.

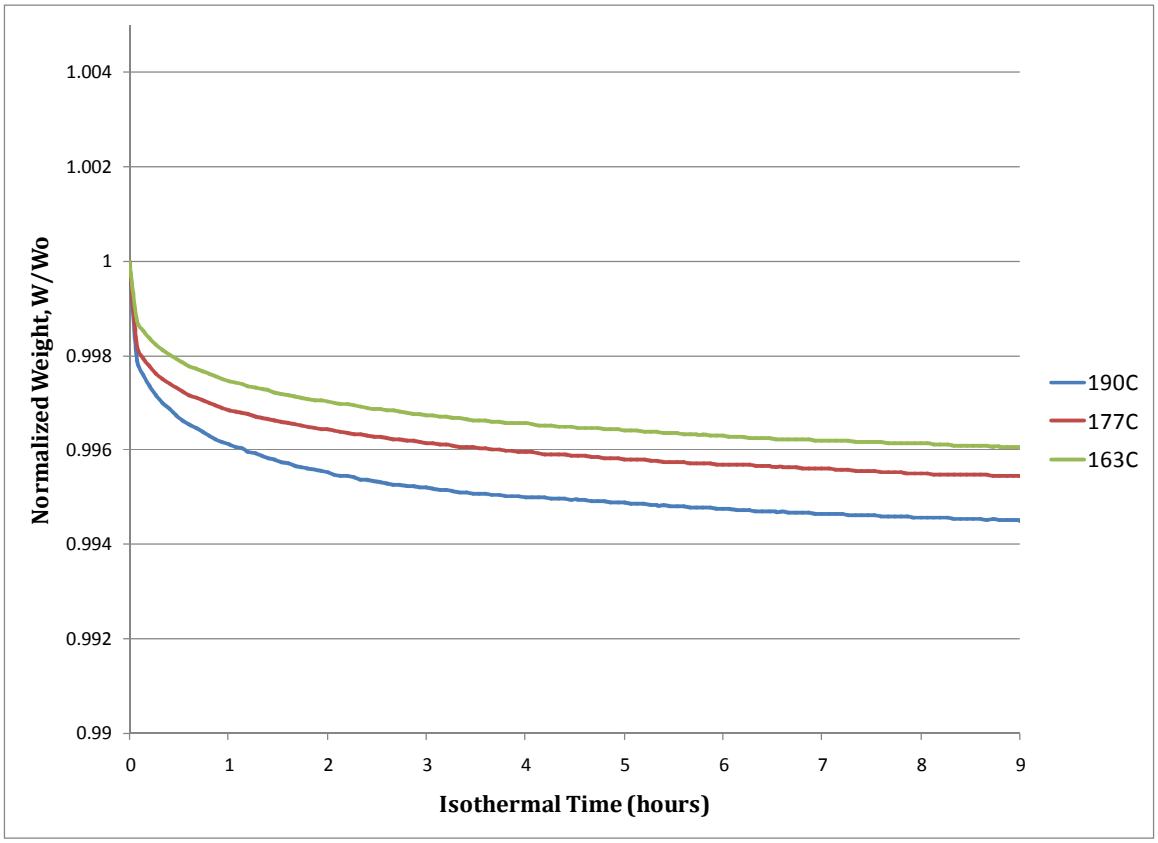

Figure 6: Initial Weight Loss of 5250-4 in Argon

The initial weight loss may be attributed to water and other volatiles given off as a result of hydroperoxide decomposition as described in the initiation (I) step of the oxidation scheme in the *Theory* chapter. Initially, hydroperoxides could have been formed from residual oxygen in the powdered 5250-4 introduced during storage. Given the large surface area of a powder, it is likely that not all oxygen was purged from the 5250-4 by argon prior to the start of the test. However, without an oxygen environment to replenish them, the hydroperoxides would soon be depleted, and the weight loss mechanism would cease. A small amount of hydroperoxides could have also been added from the processing of the 5250-4 powder. Indeed, the 20 hours of time allowed for carbon tetrachloride to evaporate at 49^0C may have been excessive, and could have increased the concentration of hydroperoxides in the polymer network. Another possible explanation for this weight loss is that it has nothing to do with hydroperoxide decomposition. Instead, a small quantity of thermally unstable hydrocarbons in the powder may be going through thermolysis. This type of process would be completely anaerobic. Regardless of the mechanism, the very low weight loss indicates that non-oxidative weight loss in 5250-4 is negligible.

The test results in argon, particularly late in each test, exhibit a considerable amount of noise. Some fluctuation in weight could be due to pressure fluctuations of either the argon gas or the nitrogen purge gas for the furnace. However, since this noise is not present in the early portions of each test, it probably is not solely the result of errors introduced by the instrument or purge gas set up. As Boyd noted (16), material properties such as strength changed in 5250-4 from aging in a nitrogen environment while weight remained unchanged. The minor weight fluctuations beyond 1000 minutes

could be attributed to motion introduced by the mechanisms by which the mechanical properties of the 5250-4 are changing. The 5250-4 was dull orange after aging in the argon environment at 190^0C. The color change from its initial bright yellow indicates that the material is undergoing a chemical change.

To determine the amount of noise introduced by the experimental set up, an empty titanium basket was loaded into the TGA and aged at 163^0C for 4300 minutes. The results are shown in Figure 7.

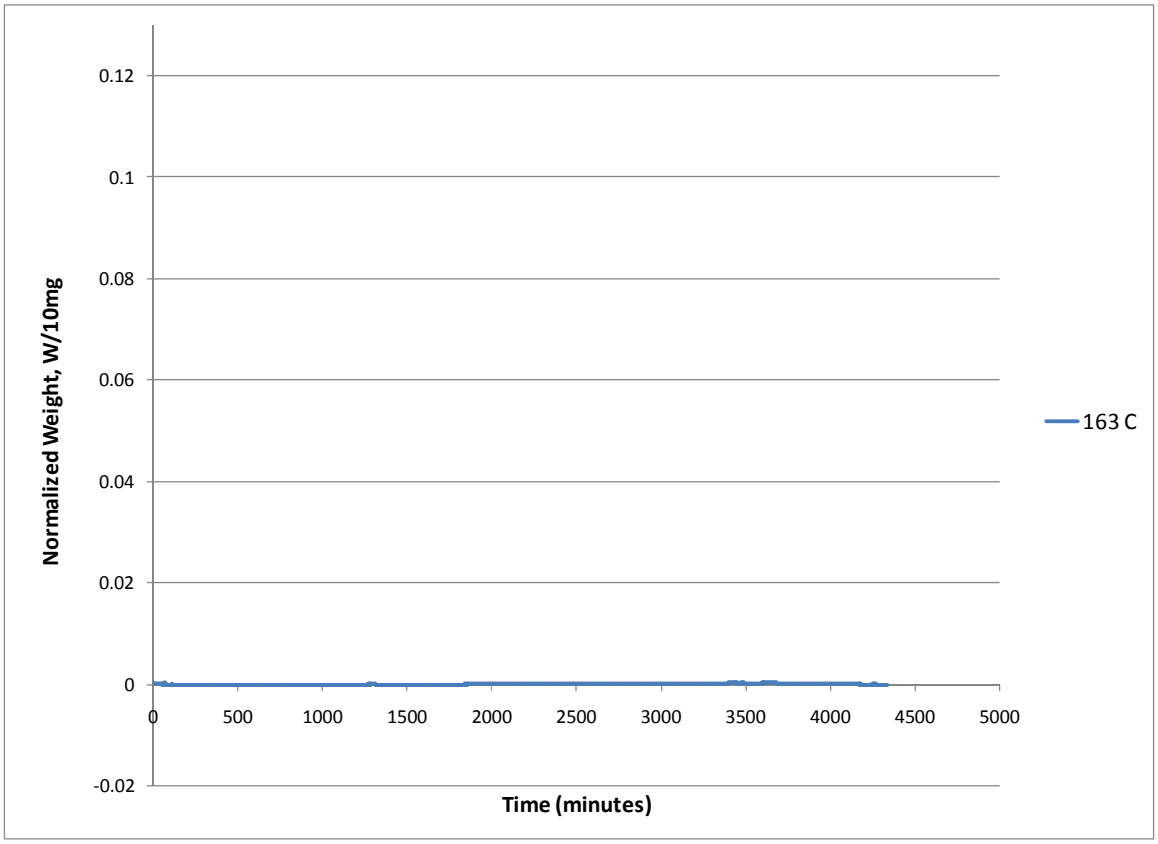

Figure 7: Indicated Weight of Empty Basket

The tare function was used to account for the weight of the titanium basket, so ideally the indicated weight should be constantly zero. The weight data was then divided

by 10 mg so that any deviation from zero would be scaled similarly to that of the errors in the data of a 10 mg 5250-4 sample. It is apparent that all of the noise in the 5250-4 argon weight loss data cannot be accounted for by TGA errors.

TGA Results in Oxygen

The second environment tested was pure oxygen, and a summary of the results of these tests are presented in Table 4 and Figure 8.

Table 4: Oxygen Test Summary

Test Temperature (^{0}C)	**163**	**177**	**190**
110^{0}C Time (min)*	120	20	12
Weight Loss at 110^{0}C*	0.32%	1.37%	0.84%
Max Weight Gain	2.59%	2.54%	1.79%
Time to Max Weight Gain (hours)	38.3	24.3	10.9
Normalized Weight after 250 hours	1.009	0.982	0.927
*Temperature of moisture evaporation hold for the 177 and 190^{0}C tests was 100^{0}C			

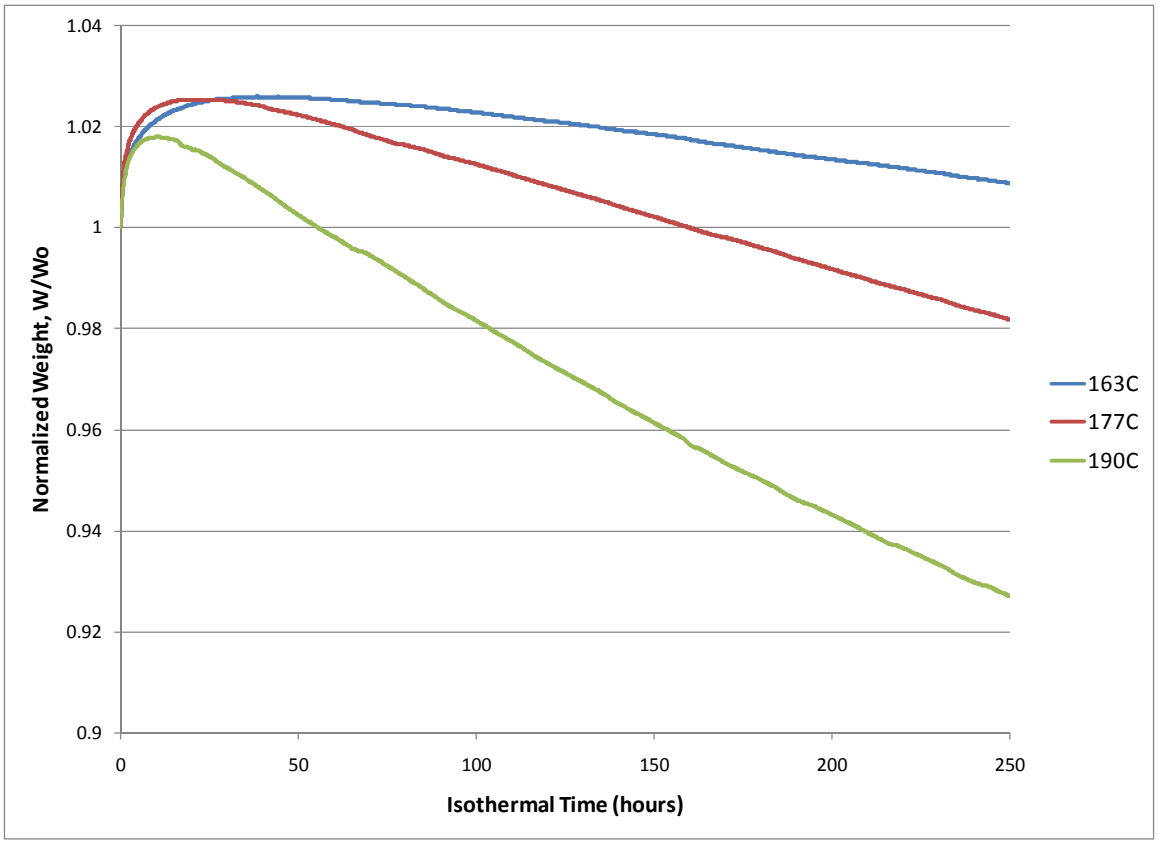

Figure 8: Gravimetric Data of 5250-4 in Oxygen

The gravimetric curves for all three tests in pure oxygen exhibit an initial period of weight gain which is in agreement with the results of thermo-gravimetric analysis of other bismaleimides. The weight gain was the highest in the 163^0C test, second highest in the 177^0C test, and noticeably lowest in the 190^0C test. The time at which the weight reached its maximum value increased with decreasing temperature. As expected, the rate of weight loss after the initial weight gain increases with increasing temperature. In fact, the rate of weight loss in the 163^0C test was so low that the test specimen still weighed more than its original weight even after 250 hours. Figure 9 shows the rate of weight loss for each temperature in oxygen. The very small scale used on this graph makes the data appear very noisy. As seen in Figure 9, the 163^0C and 177^0C data display a rate of weight loss that increases with time, indicating that a steady-state condition may not have been reached. Conversely, the 190^0C data indicate the rate of weight loss is decreasing. A decreasing rate of weight loss displayed by a BMI in an oxygen rich environment was also observed by Colin et al, and it indicates a depletion of substrate for the weight loss reaction in the polymer (7). However, the rate of weight loss did not reduce to zero by the end of 250 hours for the 190^0C test, indicating that the 5250-4 powder had not yet reached a completely oxidized state.

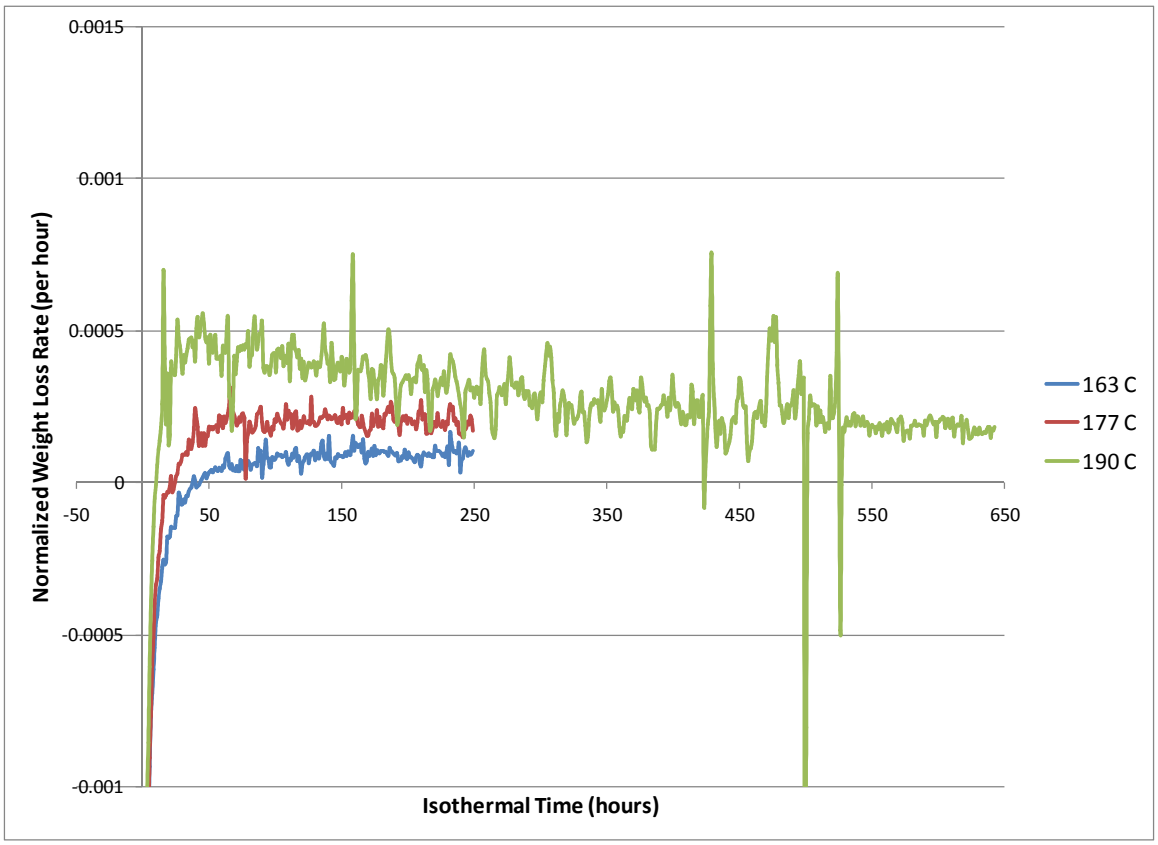

Figure 9: Rate of Normalized Weight Loss in Oxygen

Determination of φ_{ox}

The 190^0C test was extended to 645 hours (~27 days) to determine if the rate of weight loss would approach zero before the material was completely consumed. If so, the parameter φ_{ox} could be deduced. At the end of the extended test period, 83.7% of the original weight remained, but the rate of normalized weight loss was still about 0.0002 per hour. As a comparison, this rate of weight loss is similar to highest rate of weight loss of the 177^0C test. Therefore, the extended 190^0C weight loss test, showing no signs of reaching a constant weight, was terminated in the interest of time. This data does not exclude the possibility that a constant weight could be reached after longer periods of

time. The data, however, does not contradict the nanoindentation study mentioned in the *5250-4 Literature Review* of chapter one, which suggests φ_{ox} is an inappropriate parameter for 5250-4. The extended weight loss data can be found in Appendix A.

Application of Closed Loop Mechanistic Scheme

The system of differential equations described in the *Theory* section can be repeatedly solved using numeric methods until a set of parameters is obtained that provides a predicted gravimetric curve that closely matches experimental data. One problem, however, is that the number of parameters is so large that the sets of parameters to match the experimental data are not unique (26). Therefore, a number of assumptions were made to reduce the number of unknown parameters in the problem.

One such assumption is that the tests in a pure oxygen environment were in oxygen excess. When oxygen is in excess, the mechanistic scheme can be simplified by suppressing the $[P^0]$ termination steps (IV) and (V) (7). This results in neglecting rate constants k_4 and k_5. Additionally, k_2 can be assigned an arbitrarily high value because it is assumed that propagation step (II) occurs very quickly in oxygen excess (26).

Initial conditions for the set of differential equations were also assumed. As discussed in the *Theory* section, the initial concentration of hydroperoxides must be non-zero. Since the induction time for the reaction initiated by unimolecular hydroperoxide decomposition is relatively insensitive to $[POOH]_0$, it was not treated as an unknown variable. Instead it was constrained to 0.01 mol l^{-1}.

The initial concentration of substrate $[PH]_0$ was constrained to 15 mol l^{-1}, making the assumption that 5250-4 was similar in structure to another BMI of known substrate concentration (26). Additionally, for lack of oxygen solubility data on 5250-4, the value

of S was also assumed to be 3.6 x10^{-4} mol $l^{-1}Pa^{-1}$, a value corresponding to published values of other BMIs (7, 26).

The system of differential equations was solved with the ode23s stiff differential equation solver of MATLAB. Parameters for this simplified scheme were then selected to provide the best match for the experimental data. The experimental data are shown below with the numeric model in Figure 10.

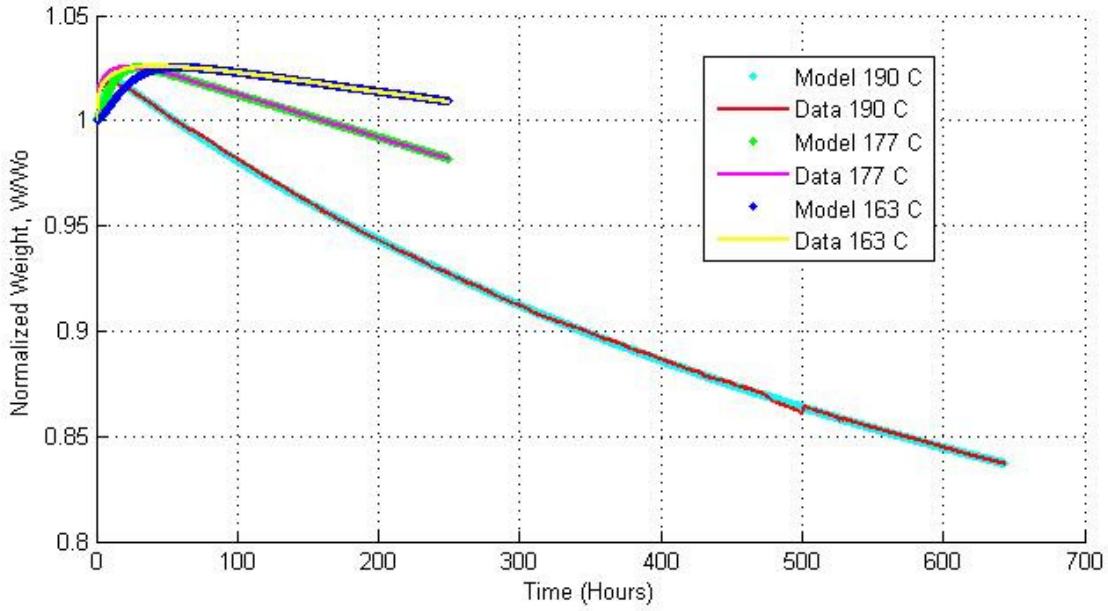

Figure 10: Normalized Weight of 5250-4 versus Time: Experimental Data and Numerical Model in Oxygen

The model fit the data well for all times except during the initial weight gain period. The data for each temperature exhibit an immediately high rate of weight gain which continually decreases to zero at the maximum weight. Conversely, the model predicts an initially small rate of weight gain, which then increases before decreasing to

zero at the maximum weight. There are a number of possibilities that may explain this difference in behavior for the 5250-4 data.

The high initial rate of weight increase suggests that the assumed initial conditions for the system of differential equations could be incorrect. As suggested earlier, small increases in the initial hydroperoxide concentration had little effect on the initial rate of weight gain. Other initial conditions that could be incorrect are the radical concentrations at time zero. It is assumed that initially the radical concentrations are zero. Inspection of equation 20 shows that weight gain results from oxygen being incorporated into the polymer. The rate of oxidation, shown in equation 21, indicates that oxygen incorporation increases as the concentration of P^0 radicals increases. Therefore, an initially high rate of weight gain could indicate an initially high concentration of radicals. However, because of their reactivity, it is unlikely that the polymer originally had a high concentration of radicals.

It may be possible that radicals were produced during the 110^0C moisture evaporation period. This short isothermal hold was intended to evaporate any water present before the test begins. It was assumed that 110^0C was sufficiently low to consider the polymer chemically static during this period. However, as seen in Figure 11, a slight increase in weight was detected during the 110^0C hold period of the 163^0C test.

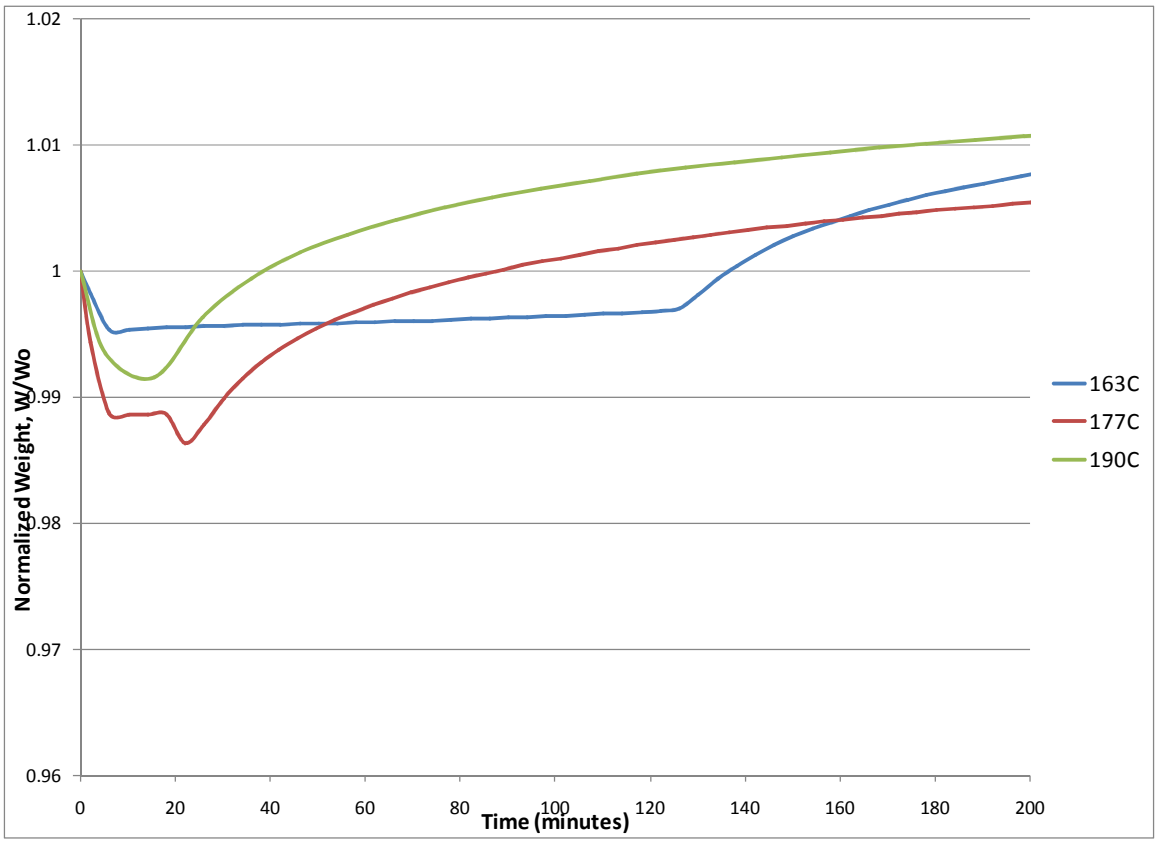

Figure 11: Moisture Evaporation Period in Oxygen

After that test, the isothermal hold time for moisture evaporation was decreased as seen in the case of the 177^{0}C and 190^{0}C tests. Additionally, the moisture evaporation temperature was decreased to 100^{0}C. However, the data still indicate a large initial rate of weight gain in the isothermal test temperature period of the 177^{0}C and 190^{0}C tests. This suggests that the 120 minute 110^{0}C moisture evaporation period was not responsible for the initial gravimetric behavior.

It is noteworthy here to mention the small weight decrease that occurred in the 177^{0}C test at 20 minutes, the time when the temperature was ramped up from 100^{0}C to the test temperature. This weight loss appears to be analogous to the non-oxidative initial

weight loss experienced by 5250-4 powder in argon. This weight loss also occurred for the 190^{0}C test, however because that test was conducted over such a long period of time, the resolution was automatically decreased. These weight loss periods are not indicated in Figure 8 because they were limited to the time period of the temperature ramp, and the weights indicated in Figure 8 were normalized by the weight at the onset of the test temperature isothermal hold. In the case of the 163^{0}C test, the weight loss was not present during the ramp up to the test temperature, presumably because it had already occurred, but was masked by the increase in weight caused by oxygen incorporation.

Another assumption that was made has to do with the basic mechanistic scheme. It is assumed that radicals are only produced by the decomposition of hydroperoxides, as opposed to radicals being formed when other polymer bonds break. If radicals are also being formed by a process that does not involve hydroperoxide decomposition, it could result in an immediate increase in radicals with temperature. It is conceivable that the brief non-oxidative weight loss observed in argon is accompanied by the production of radicals. If this is the case, tests in oxygen would exhibit a brief period of weight gain greater than predicted by assuming radicals are only produced by hydroperoxide decomposition.

Kinetics Parameters

Aside from the initial weight gain period, the model was able to match the weight loss curves for all times. This allows for r_0, the saturation reaction rate, to be determined from the relation between k_3 and k_6 shown in equation 45 of the *Theory* chapter. The parameters used in the model that gave the best fit for the experimental data are presented in Table 5.

Table 5: Kinetics Parameters for O_2

Temperature (^oC)	163	177	190
$\mathbf{k_1}$ (s^{-1})	3.00 x 10^{-5}	5.89 x 10^{-5}	12.88 x 10^{-5}
$\mathbf{k_2}$ ($l\ mol^{-1}s^{-1}$)	2 x 10^8	2 x 10^8	2 x 10^8
$\mathbf{k_3}$ ($l\ mol^{-1}s^{-1}$)	8.42	12.16	16.02
$\mathbf{k_6}$ ($l\ mol^{-1}s^{-1}$)	3.80 x10^8	4.01 x10^8	4.20 x10^8
$\mathbf{[PH]_0}$ ($mol\ l^{-1}$)	15	15	15
$\mathbf{[POOH]_0}$ ($mol\ l^{-1}$)	0.01	0.01	0.01
$\mathbf{r_0}$ ($mol\ l^{-1}s^{-1}$)	4.19 x10^{-5}	8.29 x10^{-5}	13.7 x10^{-5}
$\boldsymbol{\nu M_v}$ ($g\ mol^{-1}$)	46.90	47.00	47.29
$\boldsymbol{\gamma}$	-1	-1	-0.96

According to Colin (7), is possible to find other pairs of k_3 and k_6 that represent the long term rate of weight loss of the data well. However, it is the ratio of k_3^2/k_6 that determines r_0, and there are presumably few values of this ratio that produce an acceptable fit. Figure 12 is a plot of the natural log of the rate constants against the inverse of temperature. The linearity of this plot indicates that the rate constants in Table 5 have an Arrhenius relationship with temperature which is expected. The average molecular weight of volatiles parameter was nearly constant for the three temperatures.

According to Torrecillas et al, other than water, most of the degradation products of bismaleimides are CO and CO_2 (17). Colin et al agree that CO_2 is most prominent, but suggest that other slightly larger molecules such as C_6H_6 could be present (7). The value of νM_v determined for 5250-4 was around 47 $g\ mol^{-1}$, which is similar to the molecular weight of CO_2 (MW=44).

The parameter γ, intended to represent substrate depletion after long times, increased for the highest temperature test. The value of γ for the 190^{0}C test allows for

the apparent decrease in rate of weight loss. Longer tests might be necessary to refine the value of γ for lower temperatures.

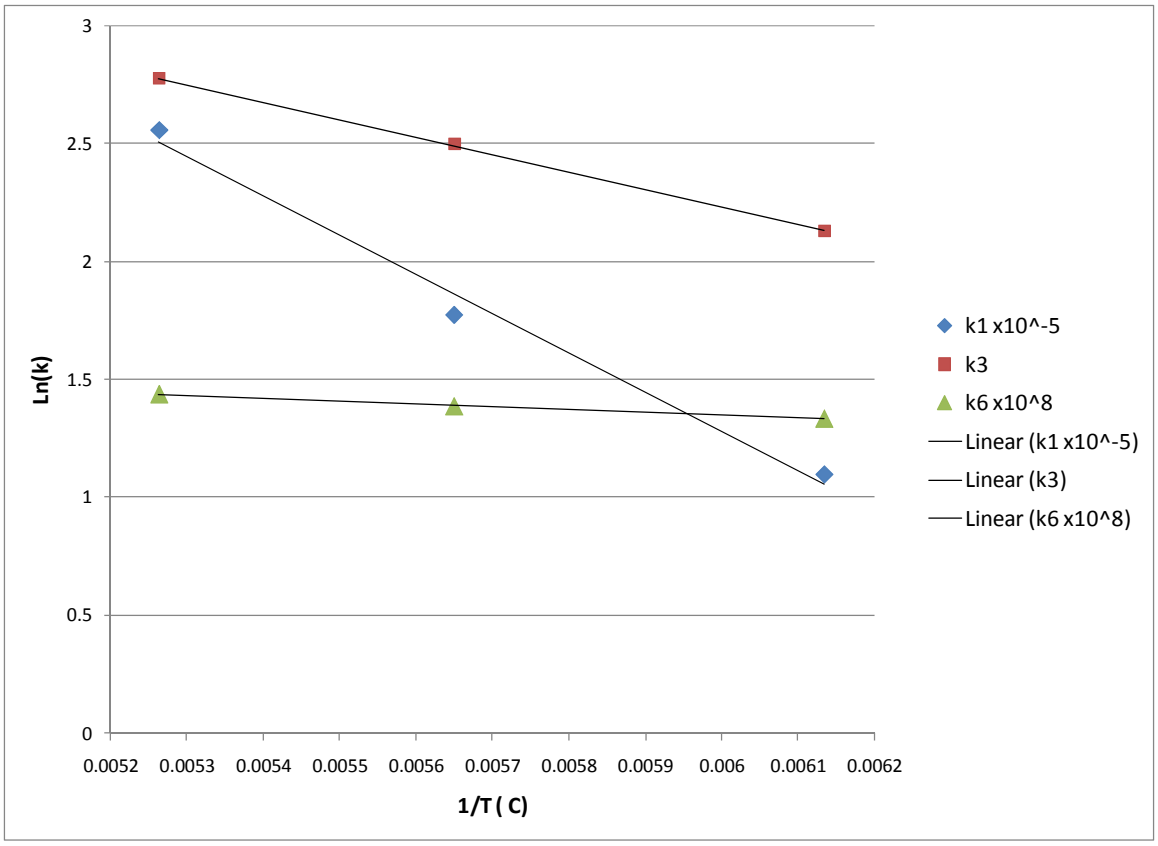

Figure 12: Temperature Dependence of Rate Constants

Application of Equivalent Property Time

The concept of equivalent property time was applied to the weight loss data of 5250-4 in pure oxygen with limited success. The difficulty of equivalent property time application to this data is due to the non-monotonous shape of the weight loss curves. Equivalent property time represents the time at which a particular conversion is reached at a given temperature using the time required to reach the same conversion at a reference temperature. In this case, conversion was defined as weight loss. As a consequence of the initial weight gain periods, each temperature thus exhibits a negative conversion

before returning to its original weight. Additionally, because the maximum weight gained at each temperature was different, conversions at one temperature may never be reached at another temperature. The result, as seen in Figure 13, is prediction curves that are skewed by the different initial weight gains.

In the first application of equivalent property time, the 190^0C data was used for the reference curve. The value for E/R, the effective activation energy, was calculated using the 190^0C and 177^0C data, and measuring the slope of ln(t) versus 1/T for the final weight of the 177^0C test. Figure 13 shows the real curves for 177^0C and 163^0C tests compared to the representations using the 190^0C data as the reference data.

As can be seen, the prediction curves for 177^0C and 163^0C underestimate the initial weight gain of the 5250-4 sample. This is because the initial weight gain of 5250-4 at the reference temperature, 190^0C, was much lower than that of the other two tests. The final weight of the 177^0C prediction matches the final weight of the 5250-4 specimen because the 177^0C test was used in conjunction with the 190^0C data for calculating the E/R parameter.

The weight predicted by equivalent property time for 250 hours at 163^0C matches the 163^0C data at 250 hours. However, this prediction was made assuming the activation energy was constant over all values of weight loss. Instead, it could vary with conversion as noted by Budrugeac (9). In this case, if the activation energy was constant, the 177^0C prediction would match the 177^0C data perfectly, at least for the portion of the weight curve under unity.

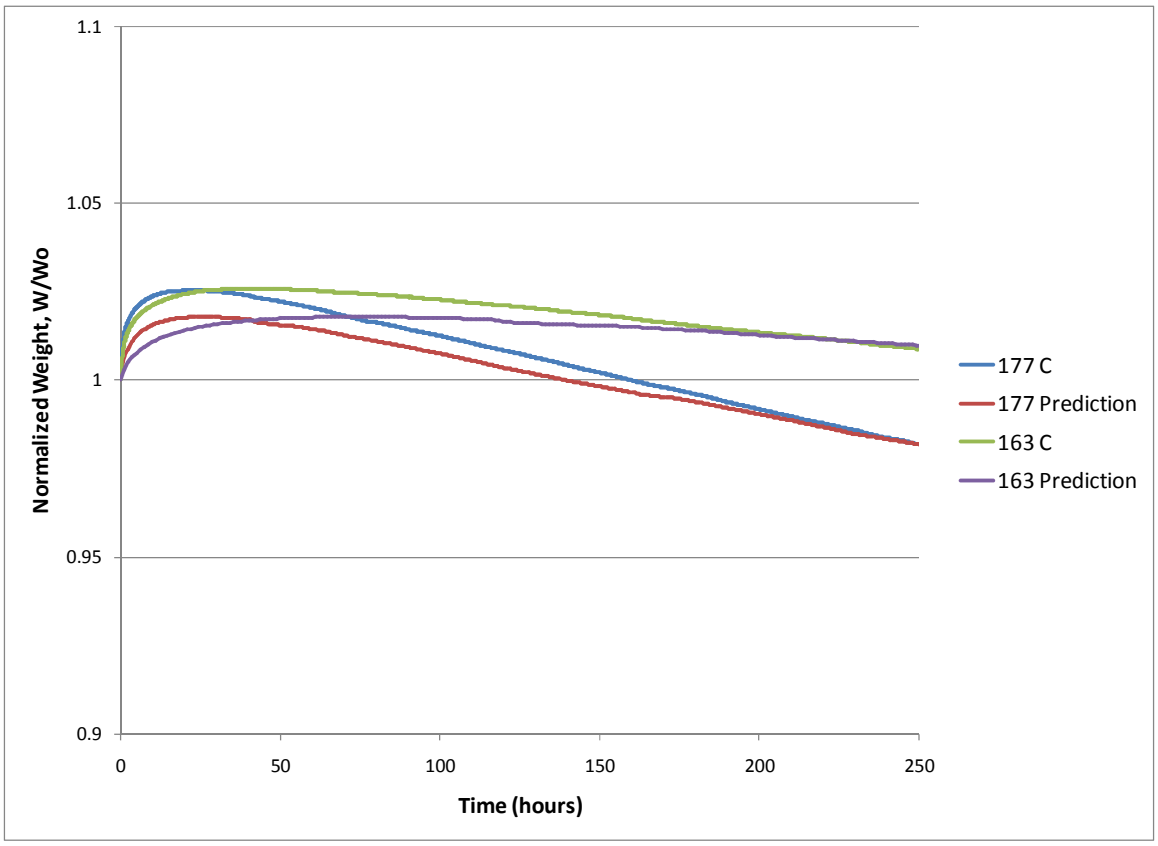

Figure 13: Application of EPT in Oxygen with 190^0C as a Reference Temperature

To investigate the effect of letting activation energy vary as a function of weight loss, E/R was determined for all weight loss values under unity. For the portion of the reference curve that was decreasing in weight but had not yet returned to its starting value, E/R was estimated by defining conversion as the percentage of weight lost between the maximum weight and weight equal to one. The plot of E/R as a function of normalized weight is seen in Figure 14.

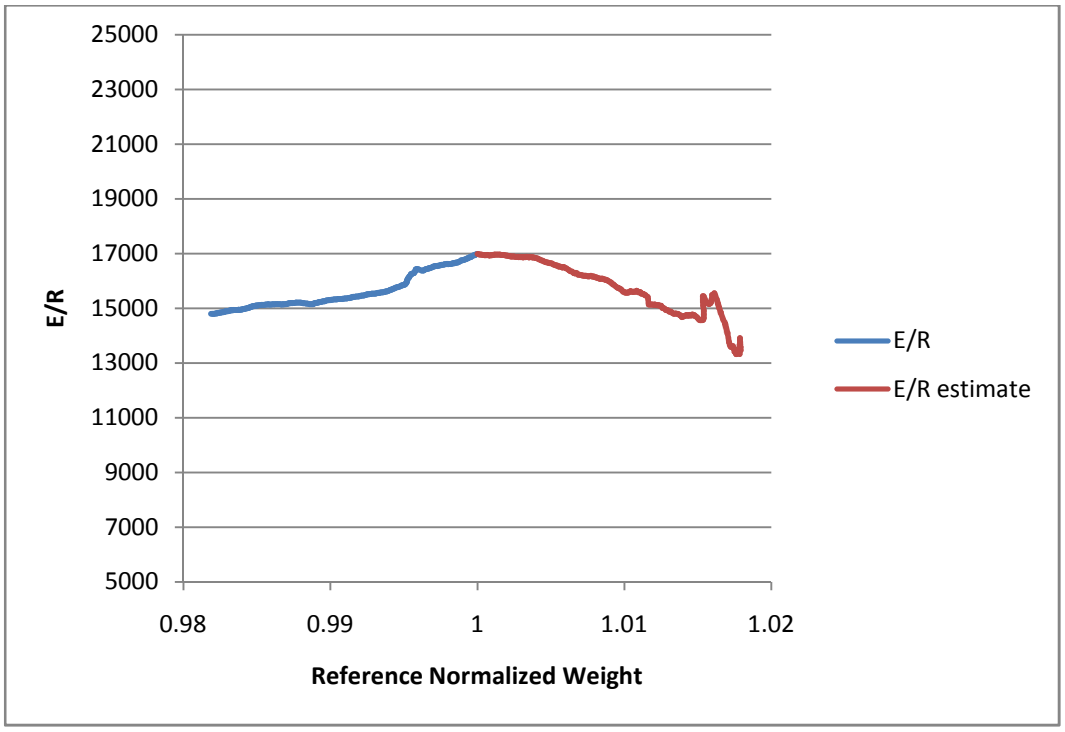

Figure 14: E/R as a function of Reference Normalized Weight

By applying E/R as a function of weight to the equivalent property time method, the prediction for the 163^{0}C gravimetric curve is not improved as seen in Figure 15. The 163^{0}C prediction curve was extended to 750 hours, and it clearly does not indicate the same rate of weight loss of the 163^{0}C data. The ability of Figure 13, using the 190^{0}C data as a reference, to predict the weight of the 163^{0}C 5250-4 test sample at 250 hours is coincidental. This may indicate a difference in activation energy between 190^{0}C and 163^{0}C.

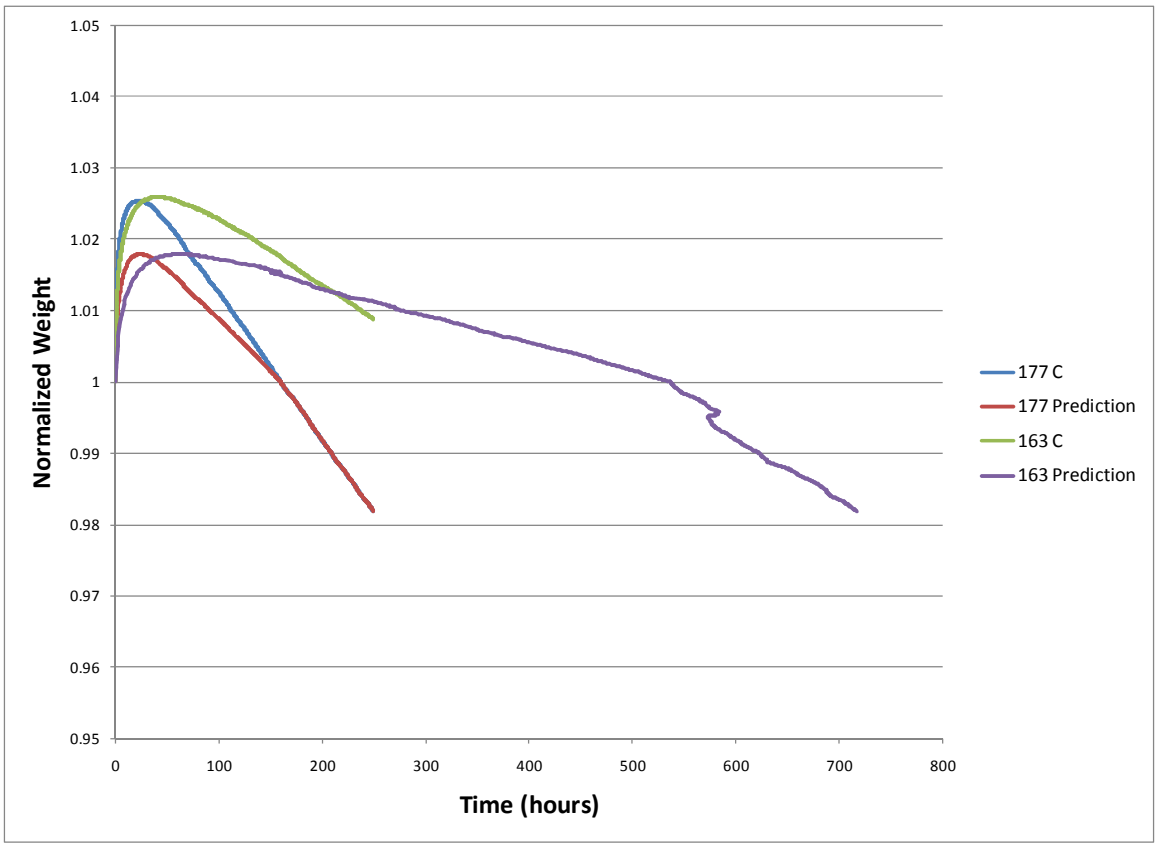

Figure 15: Application of EPT with E/R as a Function of Weight

To determine if better results could be obtained by using a lower temperature as the reference curve, it was attempted to horizontally shift the 163^0C data and 190^0C data to coincide with the 177^0C data on a weight versus log time chart. This plot is displayed in Figure 16. It is clear that the 163^0C data can be collapsed to the 177^0C data. Not surprisingly, the 190^0C curve could not be superimposed onto the 177^0C curve, indicating that equivalent property time cannot be applied to this temperature using lower temperatures as a reference curve.

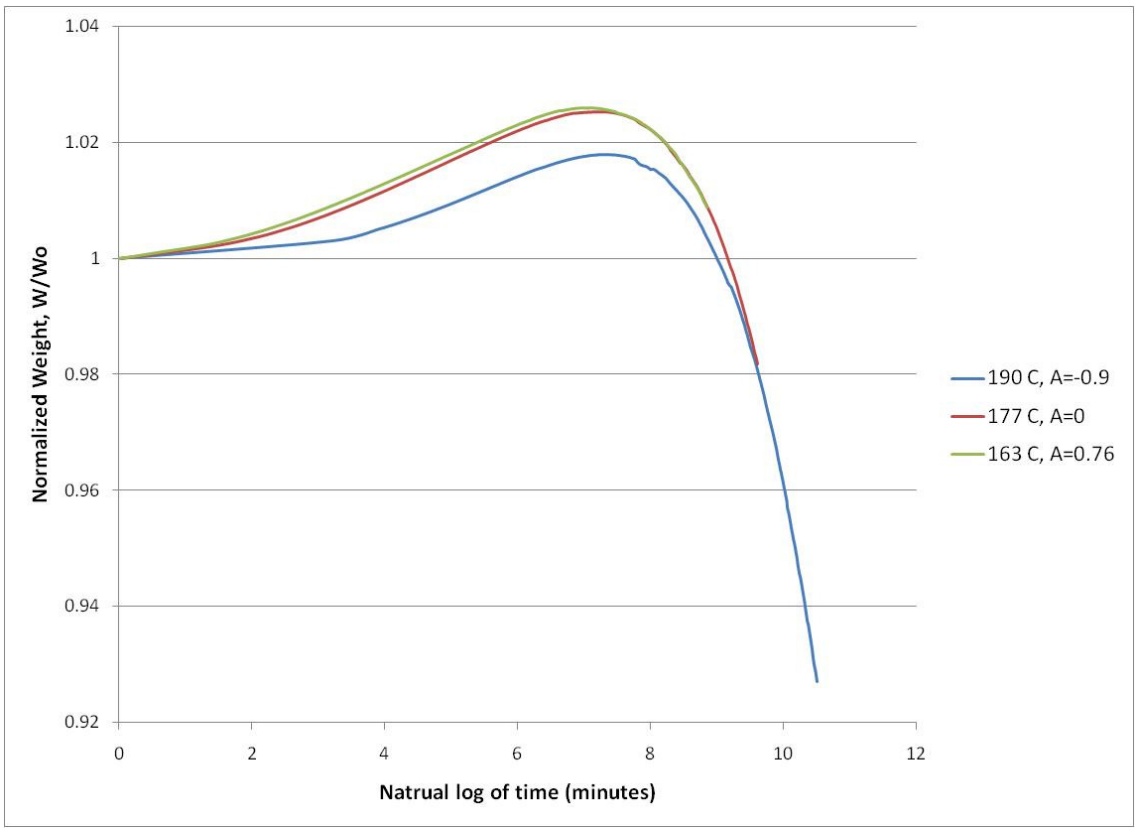

Figure 16: Time Temperature Superposition in Oxygen

Figure 17 shows the estimated gravimetric curves of the 163^0C test and the 190^0C test along with their corresponding data, using the 177^0C data as the reference curve. The predicted curve for the 163^0C data is very accurate while the 190^0C predicted curve is not very accurate. It is important to note that the shift factors A_i used in the production of Figure 16 form a linear relationship with the difference between the inverse of temperature and the inverse of the reference temperature.

$$\frac{A_i}{\left(\frac{1}{T_i} - \frac{1}{T_{ref}}\right)} = \frac{E}{R} \approx \text{constant} \tag{54}$$

However, EPT was still not able to reproduce the gravimetric curve for the 190^{0}C data. Perhaps if more data was collected for the 177^{0}C reference curve, the 190^{0}C data and the EPT representation of the curve would converge at longer times.

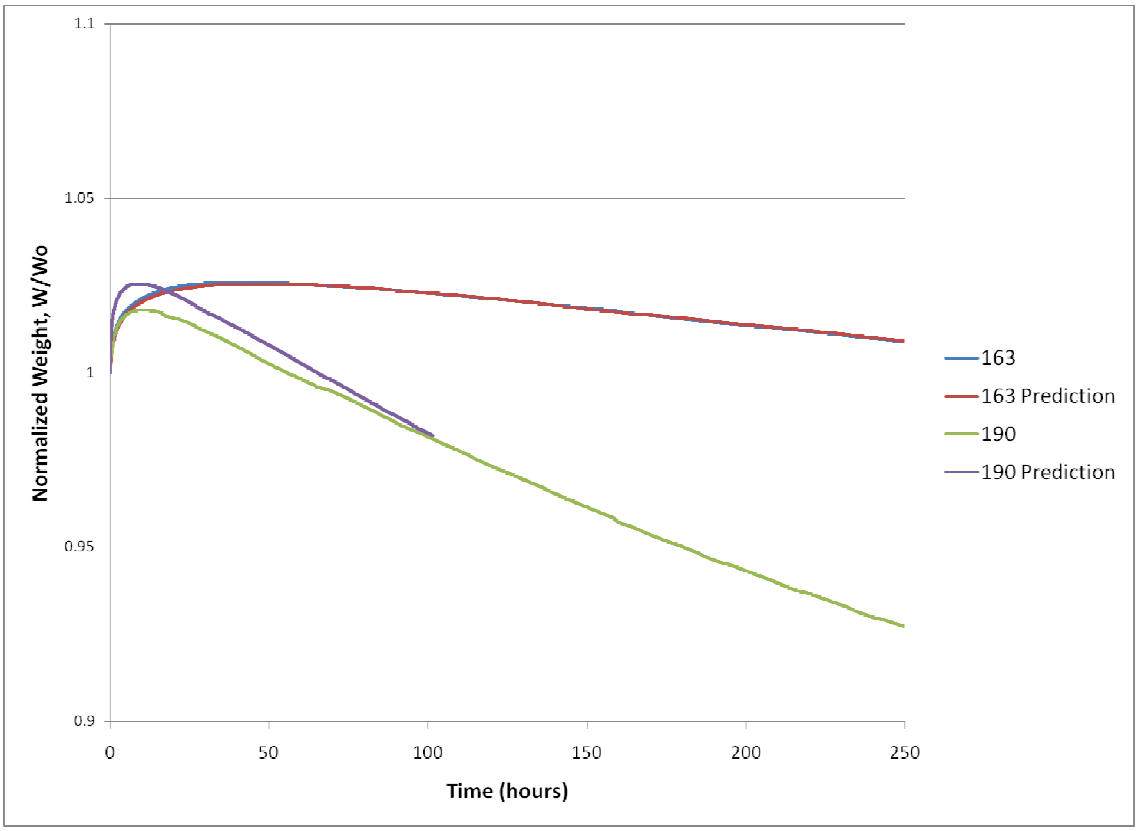

Figure 17: Application of EPT in Oxygen with 177^{0}C as a Reference Temperature

TGA Results in Air

The final environment tested was air, and a summary of the results of these tests are presented in Table 6. Plots of all three tests can be seen in Figure 18.

Table 6: Air Test Summary

Test Temperature (^{0}C)	163	177	190
110^{0}C Time (min)	60	60	60
Weight Loss at 110^{0}C	1.77%	2.10%	1.69%
Max Weight Gain	2.32%	1.96%	1.8%
Time to Max Weight Gain (hours)	134	51	24
Normalized Weight after 250 hours	1.022	1.008	0.985

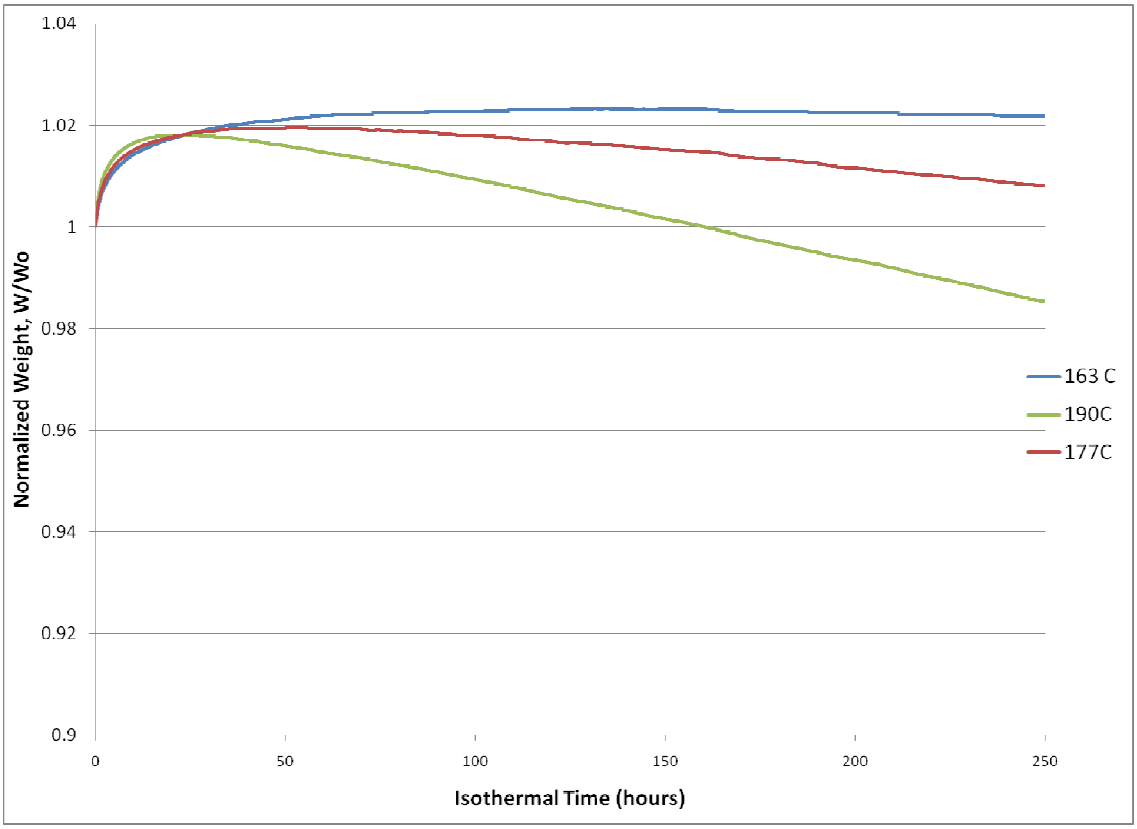

Figure 18: Gravimetric data of 5250-4 in Air

Like the results in pure oxygen, the 5250-4 polymer powder aged in air exhibit an initial period of weight gain. Again, the maximum weight gained was highest in the 163^{0}C test, and lowest in the 190^{0}C test, and the time it took to reach the maximum weight decreased with increasing temperature.

The 190^{0}C test resulted in the lowest normalized weight after 250 hours, indicating that only 1.5% of the original weight of the 5250-4 was lost. The 177^{0}C and

163^0C specimens had not even lost all of the initial weight gain after 250 hours with weights 0.8% and 2.2% higher than their initial values respectively.

Examination of the rate of weight loss after the maximum weight was reached reveals that none of the tests conclusively reached a constant rate of weight loss. This indicates that a steady-state condition had not yet been established. Because they had not lost any weight at the end of 250 hours, the 163^0C test and 177^0C test were extended to 416 and 445 hours respectively. The rate of weight loss for all three tests versus time can be seen in Figure 19. As can be seen, all three tests in air exhibit a much lower rate of weight loss than the tests in oxygen. Extended weight loss results can be seen in Appendix A.

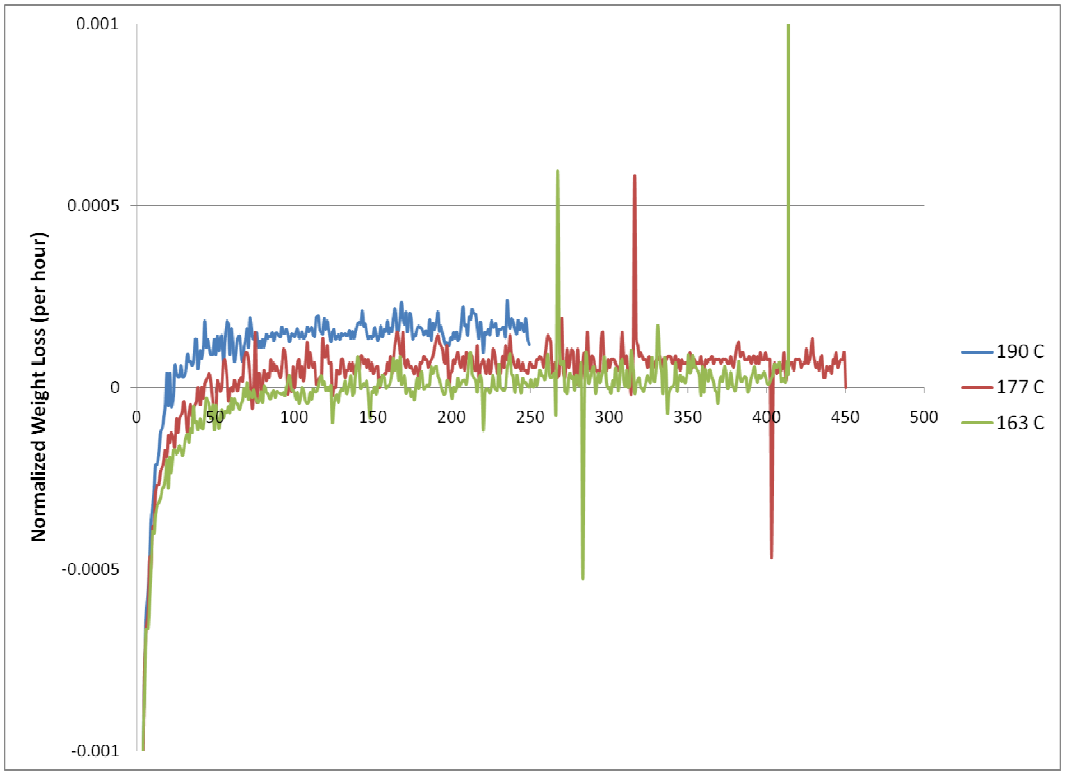

Figure 19: Rate of Normalized Weight loss in Air

With the small scale used in Figure 19, small fluctuations in the data make the rate of weight loss very noisy.

The 110^0C moisture evaporation period was held for 60 minutes for each test. As in the oxygen tests, the ramp up to the test temperature coincided with a brief period of weight loss for all three tests. This weight decrease is most likely the result of the non-oxidative weight loss exhibited in the early part of the argon data. However, as was the case in the oxygen tests, the weight loss was limited here to the ramp up to the test temperature. By the time the isothermal test period started, the oxidative weight increase had already masked any additional anaerobic weight loss. The moisture evaporation period for all three tests in air can be seen in Figure 20.

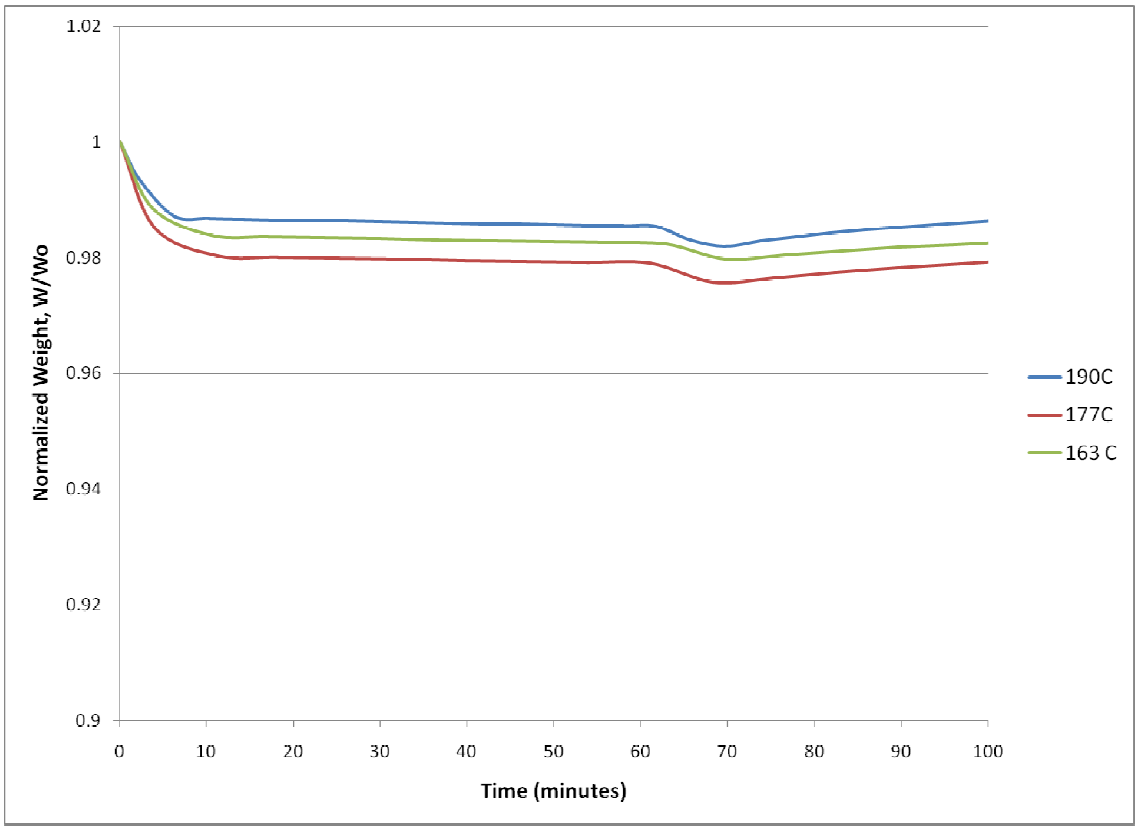

Figure 20: Moisture Evaporation period in Air

Application of Closed Loop Mechanistic Scheme

The application of the system of differential equations based on the closed loop mechanistic scheme did not produce satisfactory results for the tests conducted in air. Air, having a lower concentration of oxygen than pure oxygen, requires the inclusion of termination steps (IV) and (V). These steps account for termination reactions of $[P^o]$ that do not react with oxygen, which are considered to be negligible when oxygen is in excess.

Initially, the rate constants k_1, k_3, and k_6 determined in the oxygen excess case were applied to modeling the gravimetric curves of 5250-4 in air. This was done assuming the rate constants were functions of temperature alone, and not affected by varying the partial pressure of oxygen. Values for the rate constants k_2, k_4, and k_5 were then sought to produce weight loss curves to match those of the tests in air. Part of the difficulty of matching the model to the data in air was the very low levels of weight lost in the test period. In the case of oxygen, the model was not able to predict the beginning of the gravimetric curves as well as it could in the long term. As for the tests in air, only the 190^0C and 177^0C tests exhibited enough weight loss beyond the problematic weight gain period to apply the model. Even then, the quality of the match was poor.

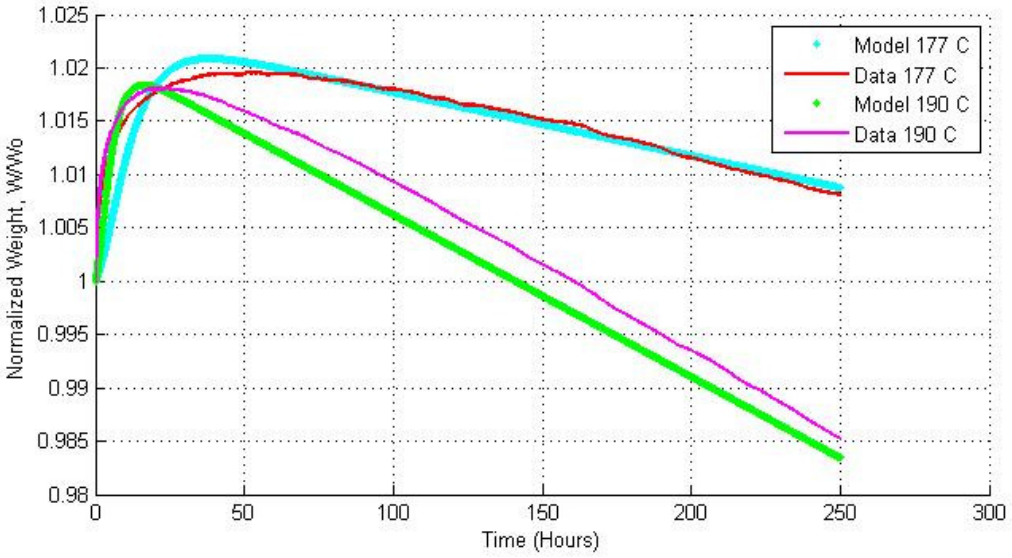

Figure 21: Normalized Weight of 5250-4 versus Time: Experimental Data and Numerical Model in Air

The kinetics parameters used to produce the model curves in Figure 21 are shown in Table 7. The fit between the experimental data and the model was improved by lowering the molecular weight and yield term νM_v by about 1%. It is possible that constituents of the air, such as water vapor, have altered the kinetics from those observed in the case of pure oxygen. This may account for a change in volatile makeup and yield. It is also possible that the rate constants themselves may take on different values in air, as opposed to a pure oxygen environment with a lower pressure. However, it is more likely that longer tests in air would be needed to produce a realistic set of kinetic parameters. Fitting the differential equations to a polymer sample that has only lost 1.5% of the original weight in one case, and not lost any weight in the other case, is not a reliable method for characterizing long term weight loss.

Additionally, the exact value of oxygen solubility in 5250-4 is necessary to determine the rate constants related to the oxygen concentration dependability when oxygen is not in excess. This value was not as important in the case of oxygen excess.

Table 7: Kinetics Parameters in Air

Temperature (^{0}C)	**163**	**177**	**190**
$\mathbf{k_1}$ (s^{-1})	--	5.7×10^{-5}	12.9×10^{-5}
$\mathbf{k_2}$ ($l\ mol^{-1}s^{-1}$)	--	2×10^{8}	2×10^{8}
$\mathbf{k_3}$ ($l\ mol^{-1}s^{-1}$)	--	10.2	15
$\mathbf{k_4}$ ($l\ mol^{-1}s^{-1}$)	--	1×10^{11}	1.5×10^{11}
$\mathbf{k_5}$ ($l\ mol^{-1}s^{-1}$)	--	2.59×10^{9}	2.73×10^{9}
$\mathbf{k_6}$ ($l\ mol^{-1}s^{-1}$)	--	4.0×10^{8}	4.30×10^{8}
$\mathbf{[PH]_0}$ ($mol\ l^{-1}$)	--	15	15
$\mathbf{[POOH]_0}$ ($mol\ l^{-1}$)	--	0.01	0.01
$\nu\mathbf{M_v}$ ($g\ mol^{-1}$)	--	46.4	46.4
γ	--	-1	-0.96

Application of Equivalent Property Time

The concept of equivalent property time was applied to results in air to determine if it was a valid method of interpolating gravimetric curves for the test temperatures considered. The highest temperature tested, 190^0C, was used as the reference temperature. This means that predictions were produced by shifting each weight data point for the 190^0C test on the time axis by an amount determined by the activation energy and the difference between the inverse of the reference temperature and the temperature of interest (equation (53)).

The activation energy parameter E/R was calculated by finding the slope of the ln(t) versus 1/T line between 177^0C and 190^0C at the final weight in the 177^0C data. As a consequence of using the 177^0C and 190^0C data to calculate the activation energy, the 177^0C prediction inevitably corresponds to the data for latter part of the curves. The

predictions of the 177^{0}C and 163^{0}C gravimetric curves are plotted with their corresponding data in Figure 22.

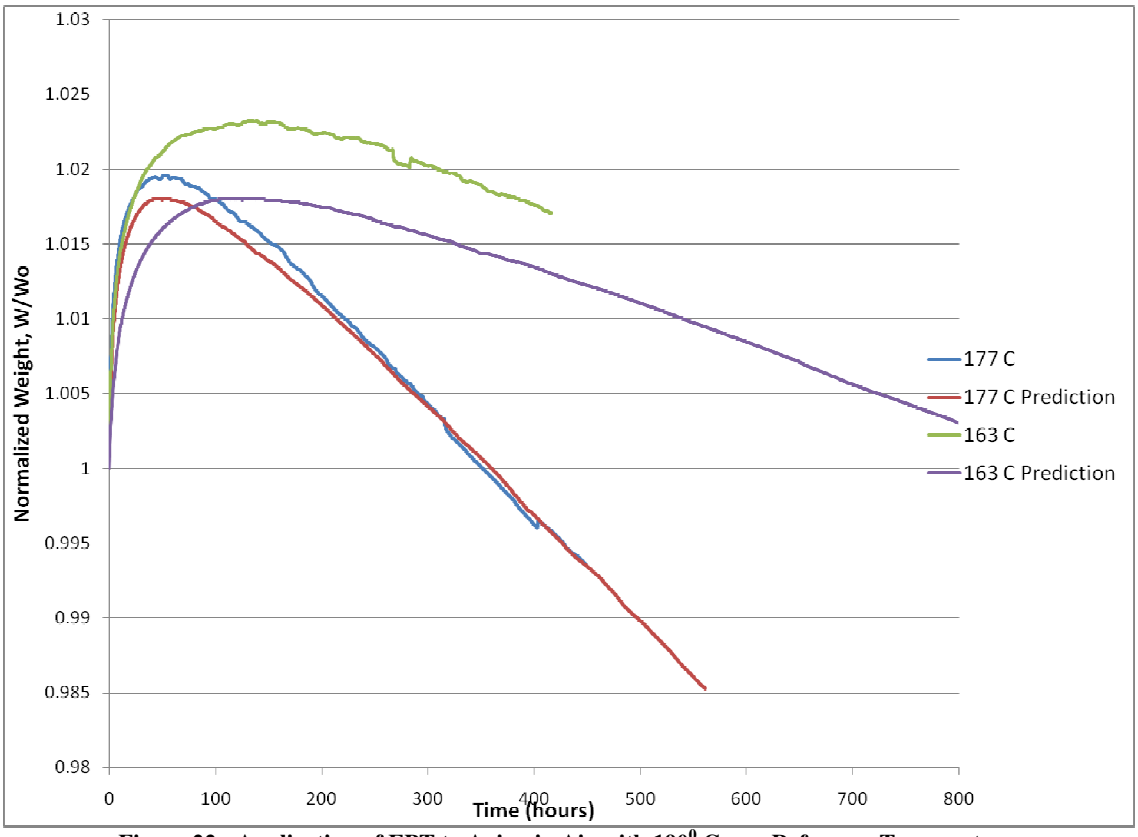

Figure 22: Application of EPT to Aging in Air with 190^0 C as a Reference Temperature

As was the case in oxygen, the different maximum weights of each test temperature make the EPT method incapable of predicting the early part of the gravimetric curves. It is interesting to note, however, that the prediction for the 177^{0}C test corresponds to a greater portion of the weight loss curve than did the corresponding prediction curve in Figure 13. This indicates that that the activation energy does not vary with weight loss as it appeared to in the case of oxygen.

After 400 hours, the weight of the 163^{0}C test sample was still too high to be predicted by shifting the 190^{0}C curve. The 163^{0}C prediction does, however, appear to be approaching the empirical data in a fashion analogous to convergence of the 177^{0}C prediction and its corresponding data. A longer test at 163^{0}C, on the order of 1000 hours, would be necessary to determine if the long term weight loss of 5250-4 in air can be predicted by applying the concept of equivalent property time to a set of reference data.

Comparison of Weight Loss Behavior in different Environments

The gravimetric curves for oxygen, air, and argon are plotted together for 163^{0}C, 177^{0}C, and 190^{0}C in Figure 23, Figure 24, and Figure 25 respectively.

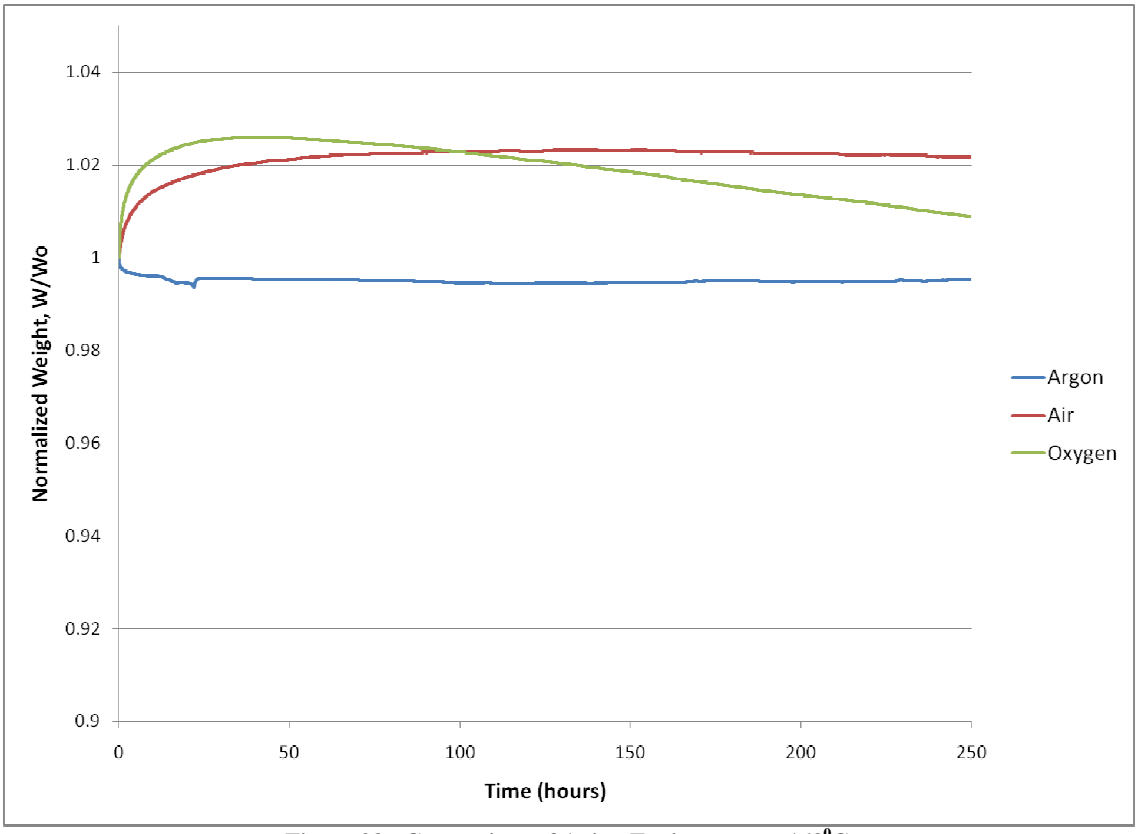

Figure 23: Comparison of Aging Environments, 163^{0}C

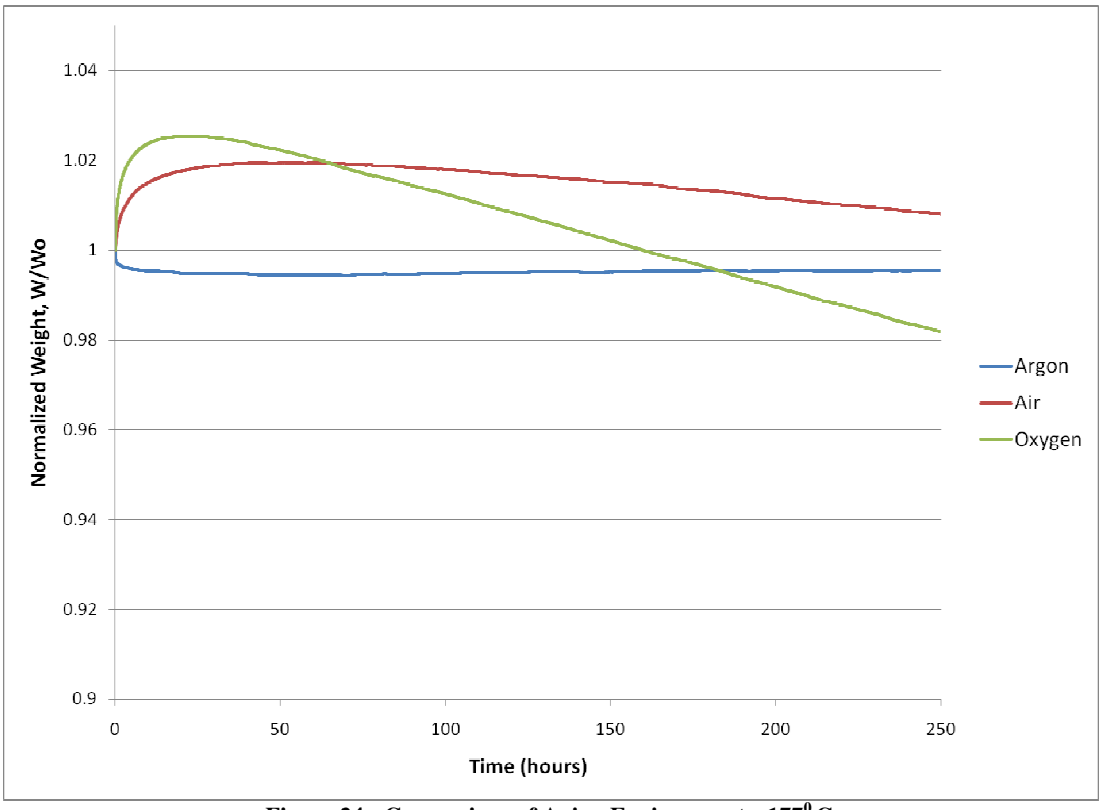

Figure 24: Comparison of Aging Environments, 177^0 C

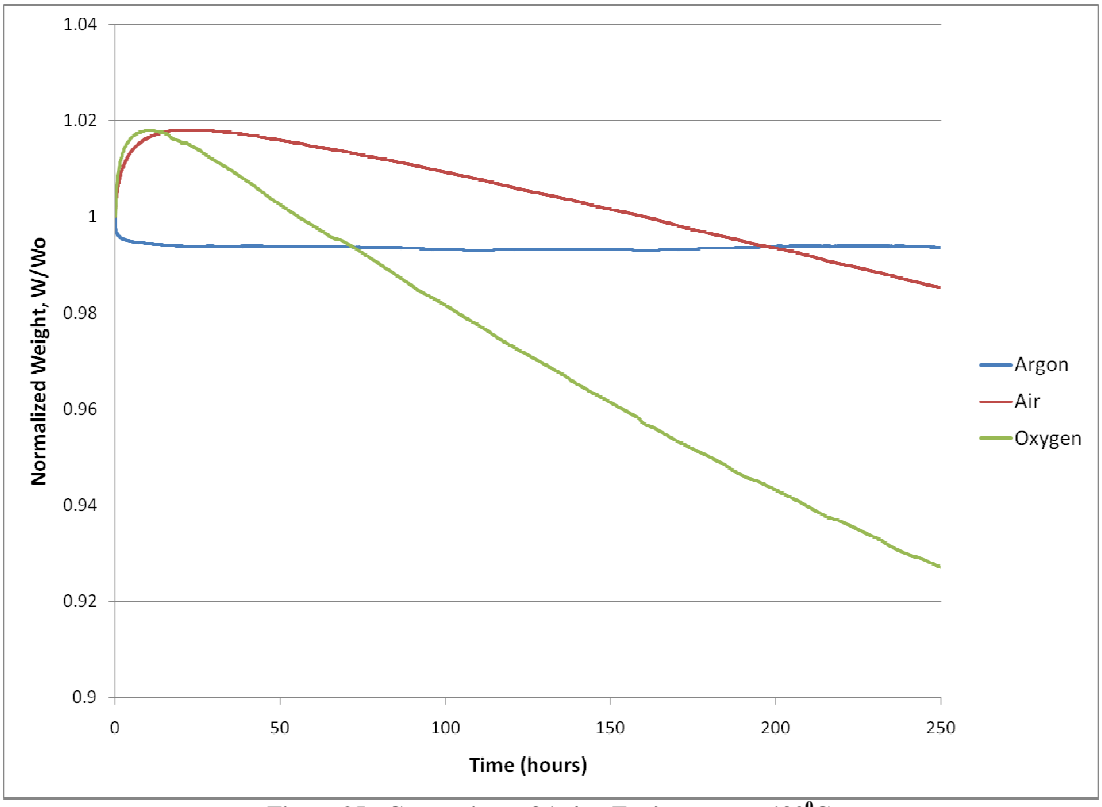

Figure 25: Comparison of Aging Environments, 190^{0}C

For all temperatures tested, the final rate of weight loss was highest for the oxygen environment and second highest in the air environment. After a small initial drop in weight, all temperatures tested in argon exhibit a near zero rate of weight loss. This supports Jack Boyd's findings that the overwhelming majority of weight loss in 5250-4 near its service temperature is the result of an oxidative process (16).

Tests in an oxidative environment show that the maximum weight gained is generally higher for a higher concentration of oxygen in the environment. This is intuitive considering the weight increase is the result of oxygen incorporation into the polymer. This can be elaborated in terms of the general oxidation scheme proposed by Colin et al (26). At higher oxygen concentrations, more alkyl radicals can react with oxygen at the rate of k_2 as seen in the first term of the rate of weight change differential equation (equation 20) and the rate of oxidation equation (equation 21). This is the term that accounts for oxygen incorporation, and therefore polymer weight gain. As time increases, the 5250-4 sample in oxygen then starts to lose weight at a greater rate than the sample in air. This is because the peroxyl radicals, formed from alkyl radical oxidation, are a reactant in the propagation step (III) that creates hydroperoxides. As the hydroperoxide concentration increases, weight loss begins to dominate via water and volatile emission as seen in the initiation step (I).

However, the tests in 190^0C indicate that the 5250-4 aged in the air environment had a higher maximum weight gain than the 5250-4 aged in an oxygen environment. This might be because the higher initiation rate constant, k_1, causes weight loss to dominate at an earlier time, thus preventing the 5250-4 sample in oxygen from reaching the same weight increase it experienced in oxygen at 177^0C. Another possible

explanation is that the parameter νM_v increases with temperature. This would indicate either larger volatile molecules are released, they are released at a greater yield ν, or a combination of both. Regardless of the cause, a higher νM_v results in a greater rate of weight loss and a shorter period of weight gain.

Parameters for AFRL Modeling Efforts

The Air Force Research Laboratory Materials and Manufacturing Directorate is interested in developing parameters for the steady state reaction rate model derived in the *Theory* chapter and repeated here.

$$\frac{dW}{dt}=\alpha R(C) \tag{55}$$

$$R(C)=2r_0\left(\frac{\beta C}{1+\beta C}\right)\left[1-\frac{\beta C}{2(1+\beta C)}\right] \tag{56}$$

The saturation reaction rate r_0 was calculated in the oxygen results section by fitting the model proposed by Colin et al to the experimental data in oxygen excess. The oxygen concentration dependence parameter β can be calculated with the method used by Pochiraju and Tandon in their research of PMR-15 (11), and later by ENS Grant Robinson in his study of PMR-15 (24). Assuming the weight loss proportionality constant (α) is independent of oxygen concentration, equation 56 applied to two different oxygen concentrations can be divided by itself. The resulting relation can be solved for the concentration parameter β.

$$\left(\frac{\beta C_1}{1+\beta C_1}\right)\left[1-\frac{\beta C_1}{2(1+\beta C_1)}\right]=\left(\frac{\frac{dW_1}{dt}}{\frac{dW_2}{dt}}\right)\left(\frac{\beta C_2}{1+\beta C_2}\right)\left[1-\frac{\beta C_2}{2(1+\beta C_2)}\right] \tag{57}$$

Using the concentration of oxygen in the polymer in air as C_1 and the concentration of oxygen in the polymer in a pure oxygen environment as C_2, β could be determined using the rate of weight loss in air ($\frac{dW_1}{dt}$) and the rate of weight loss in pure oxygen ($\frac{dW_2}{dt}$). However, the correct rate of weight loss to apply to this equation must be selected with care.

As explained in the *Theory* chapter, equation 56 is based on a number of assumptions which stem from the existence of a steady-state rate of oxidation. This would occur when the time rates of change of radicals and hydroperoxides are close to zero. If this is the case, equation 20 predicts that the rate of weight loss will be constant. Equation 56 is also based on the assumption that the substrate concentration has remained relatively unchanged. The region of data collected for 5250-4 where these assumptions are valid, therefore, corresponds to a time after a constant rate of weight loss is established and before the rate of weight loss begins to decelerate due to decreased substrate availability.

In the oxygen tests, it appears as if a steady state rate of weight loss has been reached for the 190^0C test and possibly the 177^0C test. In air, however, the rate of weight loss was still slowly increasing at the conclusion of all three tests. This was even true for the 163^0C and 177^0C tests in air, which were aged for nearly three weeks. For the tests in air, therefore, an average rate of weight loss at the conclusion of the test was used to calculate the concentration parameters β.

The rates of weight loss and the times over which they were obtained are listed in Table 8 and Table 9.

Table 8: Time Domain for Steady-State Rate of Weight Loss

	163^0C	177^0C	190^0C
Oxygen	10,000-15,000 min.	10,000-15,000 min.	3000-5400 min.
Air	9,000 min. to end	20,000 min. to end	9500 min. to end

.

Table 9: Rates of Weight Loss used in Calculation of Concentration Parameter

	163^0C	177^0C	$190\ ^0$C
Oxygen	9.38×10^{-5}	2.01×10^{-4}	4.25×10^{-4}
Air	2.28×10^{-5}	6.76×10^{-5}	1.64×10^{-4}

MATLAB was used to find the values of β which satisfy equation 57 for the ratio of weight loss rates at each of the three temperatures. The concentration of oxygen in the polymer in air was $C=7.660 \times 10^{-3}$ mol/l and the concentration of oxygen in the polymer in an oxygen environment was $C=3.648 \times 10^{-2}$ mol/l.

The weight loss proportionality constant, α, in equation 55 is used to correlate the rate of oxidation to the rate of weight loss. Using the saturation rate of oxidation (r_0) the proportionality constant can be determined from the rate of weight loss as was done in the previous study of PMR-15 by Robinson (24).

$$\alpha = \frac{\frac{dW}{dt}}{R(C)} \tag{58}$$

Recalling that the rate of weight loss used in this thesis is normalized by the original weight, the numerator has units of s^{-1} and the denominator has units of oxidation rate, mol $l^{-1}s^{-1}$ giving α units of l mol^{-1}. The rates of weight loss used to determine alpha were from the steady state time domain of the oxygen tests. In oxygen excess, the oxidation reaction rate is equal to the saturation reaction rate r_0. The calculated values of the

concentration parameters and proportionality constants for the three test temperatures are shown below Table 10.

Table 10: Parameters for AFRL Modeling Efforts

	163°C	**177°C**	**190°C**
$\mathbf{r_0}$ (mol $l^{-1}s^{-1}$)	4.19 x10^{-5}	8.29 x10^{-5}	13.7 x10^{-5}
β (l mol^{-1})	3.58	14.88	21.7
α (l mol^{-1})	6.22 x10^{-4}	6.74 x10^{-4}	8.62 x10^{-4}

For the temperatures considered, the concentration parameter β increases with temperature. This has the effect of making the oxidation reaction rate at a given partial pressure of oxygen equal to a greater percentage of the saturation reaction rate at higher temperatures than would be the case at lower temperatures. This does not necessarily mean that at higher temperatures the difference in weight loss rate between pure oxygen and air is less than the difference observed at low temperatures. The reason for this is because the saturation reaction rate and the proportionality constant are also increasing with temperature. The increase in β with temperature is a result of the ratio of weight loss rates between the air environment and oxygen environment increasing with temperature.

The effect of the air tests not reaching a constant rate of oxidation within the time of the experiment is an underestimated set of values for β. Longer testing or testing at higher partial pressures of oxygen would be required to find more accurate values. As a comparison, published values of β for another BMI (F655-2 type) are roughly four times larger than those shown in Table 10 (12).

The implications of obtaining β values as low those in Table 10 extend to the determination of r_0. The values of r_0 were determined by assuming that the tests run in an oxygen environment were in excess of oxygen, meaning that a higher concentration of oxygen would not affect the weight loss behavior. This allowed for the suppression of termination steps (IV) and (V) in the general oxidation scheme as explained in the *Results in Oxygen* section, which in turn led to the selection of rate constants k_1, k_3, and k_6 as well as the molecular weight of volatile molecules. However, β values as low as those indicated in Table 10 suggest that a pure oxygen environment at standard pressure would not provide for an oxidation rate to reach saturation levels. For example, at $\beta=21.7$ l mol^{-1}, the oxidation rate at 190^0C in the oxygen environment would have only reached 69% of the saturation reaction rate. In light of this fact, the saturation reaction rates r_0 determined in the *Results in Oxygen* section may also be underestimated. However, longer tests in air may indicate that the reported β values here are instead incorrectly low.

The values for the weight loss correlation constant α are also suspect. Although weight loss rates from the apparent steady state region of the oxygen tests were used to calculate α, an artificially low saturation reaction rate suggests the α values reported in Table 10 are too high.

V. Conclusions

Weight Loss in 5250-4 Neat Resin Powder

The aging of 5250-4 neat resin powder in argon indicated that negligible weight loss is attributed to a non-oxidative process. This result corresponds to other weight loss tests of 5250-4 bulk samples carried out in inert environments (16). However, the 5250-4 was not unchanged by the elevated temperature in argon, as indicated by its color change. Non-oxidative effects on material properties of 5250-4, which do not have a corresponding weight loss, must therefore be investigated.

The test results in oxygen and air both reveal an initial weight gain period that is common for BMIs in the presence of oxygen. The weight gain is attributed to oxygen being incorporated into the polymer at a greater rate than degradation products are being released early in the isothermal hold. Eventually, the weight loss mechanism overtakes the effects of oxygen incorporation and weight begins to decrease. The time necessary for the polymer to reach its maximum weight is temperature dependent, with 5250-4 samples reaching their maximum weight earlier for higher temperatures. The maximum weight gained also appears to be dependent on temperature, with maximum weight gained decreasing with increasing test temperature.

The total weight loss experienced by all temperatures in air and oxygen was surprisingly low. At the end of 250 hours, the 163^0C and 177^0C tests in air, as well as the 163^0C test in oxygen did not lose enough weight to compensate for the initial weight

gain. Furthermore, even with extended testing periods, it is unclear whether a steady-state constant rate of weight loss was established for the tests in air.

Application of Closed Loop Mechanistic Scheme

Under the assumption that 5250-4 is in oxygen excess in pure oxygen at standard pressure, the data for the oxygen tests were able to be described by the set of differential equations derived from a generalized closed loop oxidation scheme. The resulting kinetics parameters followed the expected Arrhenius relation with temperature. This suggests that the oxidation of 5250-4 can be described with the oxidation scheme developed by Colin et al (26). The saturation reaction rate of 5250-4 was determined from the kinetics parameters at each temperature in pure oxygen. The ability to model the results in air were less successful, most likely because of inaccurate assumptions for material properties such as the solubility of oxygen in 5250-4. Additionally, the extremely low weight loss of 5250-4 in air made it difficult to characterize long term weight loss.

Application of Equivalent Property Time

The method of equivalent property time was investigated as a possible means of producing gravimetric curves for temperatures that fall within the range of those tested. The initial weight gain period was not able to be reproduced by using a reference temperature, owing to the temperature dependence of the maximum weight gained. An attempt was made to apply equivalent property time to the end of the gravimetric curves. Applying EPT in oxygen using 190^0C data as a reference curve was unsuccessful. However, when the 177^0C data is used as the reference curve, a good representation of

the 163^0C data can be produced. In air, the 190^0C data was used as the reference curve in the application of EPT. The method provided a good representation of the 177^0C data. The quality of the fit for the 163^0C data is inconclusive owing to the fact that the 5250-4 gained the most weight at this temperature, and, even after extending the isothermal hold to 417 hours, the test was concluded before sufficient weight loss was reached.

Parameters for AFRL Modeling Efforts

Parameters for the steady-state model used by AFRL to represent polymeric weight loss in polymer matrix composites were determined from the gravimetric data. The concentration parameters (β) determined for each temperature were lower than expected because a steady-state condition was not reached in the air environment tests. The weight loss correlation parameter (α) was also determined for each temperature. However, if saturation reaction rates r_0 were underestimated due to an invalid oxygen excess assumption, the values of α presented here are overestimated.

Recommendations

The objective of this thesis was to determine weight loss parameters for 5250-4 neat resin that could be used to further characterize oxidation layer growth and overall degradation of 5250-4 composites. At the onset of the research it was assumed that the testing conditions decided upon would result in significant weight loss that would lend itself to analysis of the pertinent parameters. However, the 5250-4 powder proved to be much more resistant to weight loss than expected, even in oxidative environments. The 250 hours allotted to isothermal hold time at the investigated temperatures was not enough time to observe a steady-state rate of weight loss in many cases, and it certainly

was not long enough to observe a reduced rate of weight loss as the result of oxidation sites in the polymer being exhausted. To truly characterize the oxidative weight loss of 5250-4 requires much longer aging times or more aggressive aging conditions.

It is recommended to use oxygen at a number of increased pressures to determine the partial pressure of oxygen above which oxidation rate is no longer increased. This would allow for test conditions to be established which ensure the 5250-4 powder is being oxidized at its saturation reaction rate. Doing so can ensure that using a simplified oxidation scheme with fewer parameters is valid. Additionally, experiments should be designed to ascertain the solubility of oxygen in 5250-4 to eliminate the use of assumed values from other BMI systems.

Identifying the out-gassed degradation products would also be valuable to the modeling efforts. It would be helpful in determining how the molecular weight of degradation products changes with increasing temperature, or even if there is a difference between aging in pure oxygen and aging in air.

There were also procedural problems involved in this study. One such problem was the apparent reaction of 5250-4 during the moisture evaporation period. To minimize the effects of any such reaction, the isothermal hold time should be consistently short, and perhaps lower in temperature. Additionally, the excessively long elevated temperature hold used to evaporate carbon tetrachloride from the 5250-4 powder after suspension should be avoided.

Appendix A: Extended Weight Loss Data

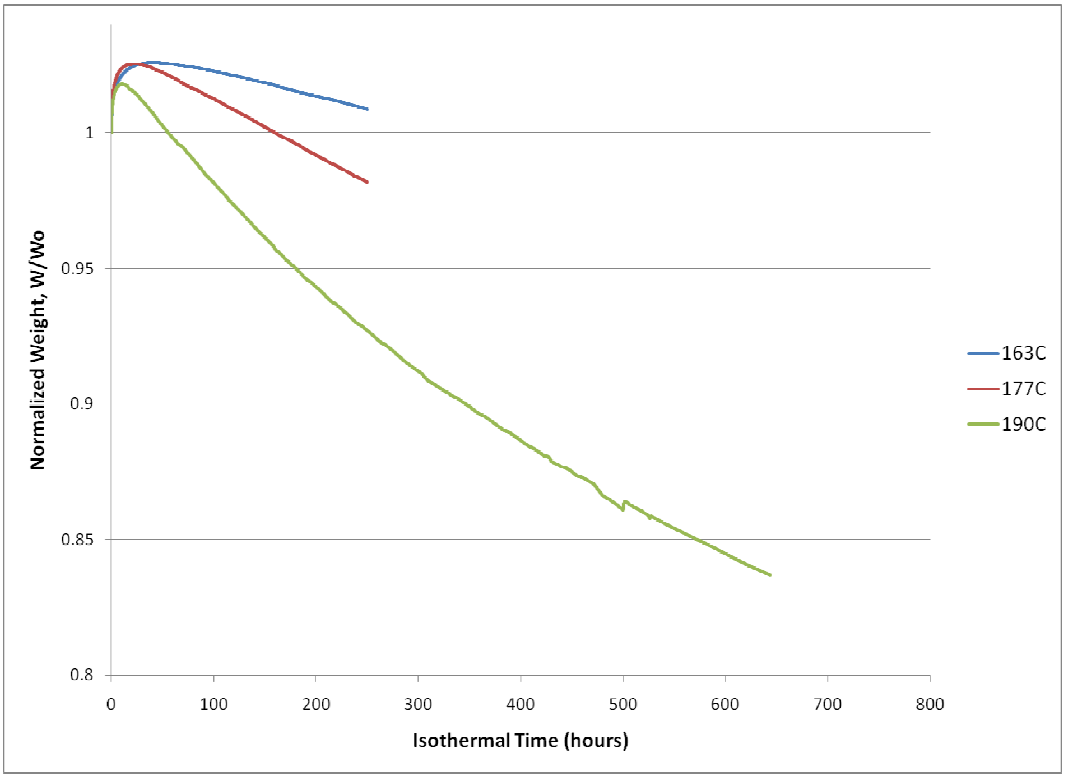

Figure26: Extended Weight Loss Curves: Oxygen

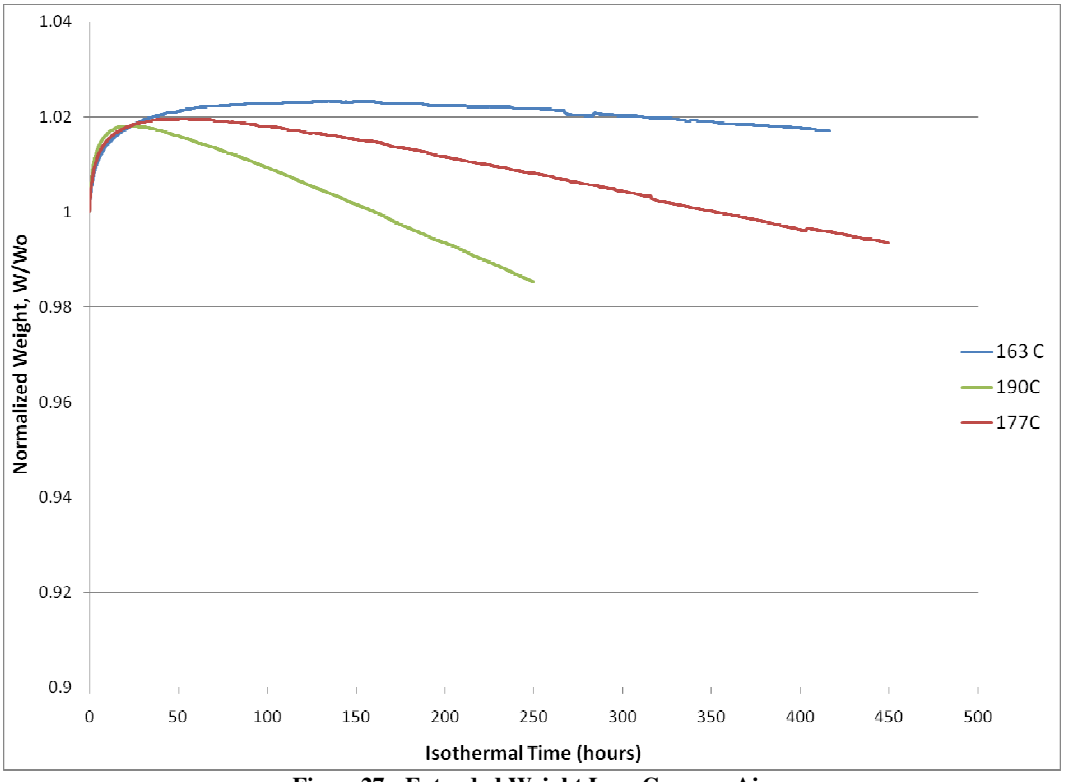

Figure27: Extended Weight Loss Curves: Air

Bibliography

1. Regnier, N. and C. Guibe. "Methodology for multistage degradation of polyimide polymer," Polymer Degradation and Stability, 55: 165-172 (1997).

2. Baker, Alan, Stuart Dutton, and Donald Kelly**.** *Composite Materials for Aircraft Structures* (2nd Edition). Reston VA: American Institute of Aeronautics and Astronautics, 2004.

3. McManus, H. L., B. J. Foch, and R. A. Cunningham. **"**Mechanism-Based Modeling of Long-Term Degradation," *Journal of Composites Technology & Research*, 22: 146-152 (July 2000).

4. Schoeppner, G. A., G.P. Tandon, and K.V. Pochiraju. "Predicting Thermo-Oxidative Degradation and Performance of High Temperature Polymer Matrix Composites," in *Multiscale Modeling and Simulation of Composite Materials and Structures*. Eds. Kwon, Y., D. H. Allen, and R. Talreja: Springer-Verlag, 2007.

5. Alves, N.M., J.F. Mano, and J. L. G. Ribelles. "Structural relaxation in a polyester thermoset as seen by thermally stimulated recover," *Polymer*, 42: 4173-4180 (2001).

6. Pascault, Jean-Pierre and others. *Thermosetting Polymers.* New York: Marcel Dekker, Inc., 2002.

7. Colin, X., C. Marais, and J. Verdu. "Kinetic Modelling and Simulation of gravimetric curves: application to the oxidation of bismaleimide and epoxy resins," *Polymer Degradation and Stability*, 78: 545-553 (2002).

8. Seferis, James C. "Aging Analyses of Polymer Composites Through Time-Temperature Equivalence," *Journal of Composites Technology and Research*, 21: 173-179 (July 1999).

9. Budrugeac, P. "Some methodological problems concerning the kinetic analysis of non-isothermal data for thermal and thermo-oxidative degradation of polymers and polymeric materials," *Polymer Degradation and Stability*, 89: 265-273 (August 2005).

10. Rodriguez-Arnold, J., F. E. Arnold, and R. E. Lyon. "Kinetics and Mechanisms of Decomposition of High Performance Polymers," *Proceeding of Fire and Materials 4th International Conference and Exhibition*. 279-287. Crystal City VA, Novermber 1995.

11. Pochiraju, K. V. and G. P. Tandon. "Modeling Thermo-Oxidative Layer Growth in High-Temperature Resins," *Journal of Engineering Materials and Technology*, 128: 107-116 (January 2006).

12. Colin, X., C. Marais, and J. Verdu. "Thermal Oxidation Kinetics for a Poly(bismaleimide)," *Journal of Applied Polymer Science*, 82: 3418-3430 (December 2001).

13. Colin, X., C. Marais, and J. Verdu. "A new method for predicting the thermal oxidation of thermoset matrices: Application to an amine crosslinked epoxy," *Polymer Testing*, 20: 795-803 (2001).

14. Bongiovanni, Christopher and Jack Boyd. "Bismaleimide Composites with 450F and Higher-use Temperature Capability," *International SAMPE Symposium and Exhibition*. 2973-2983. Long Beach: SAMPE, 2005.

15. Gray, Robert A. *Low-toxicity, high-temperatrue polyimides.* US Patent 6,184,333. 6 February 2001.

16. Boyd, Jack D. and Glenn E. C. Chang. "Bismaleimide Composites for Advanced High-Temperature Application," *38th International SAMPE Symposium*. 357-369. Anaheim: SAMPE, 1993.

17. Torrecillas, R., N. Regnier, B. Mortaigne**.** "Thermal degradation of bismaleimide and bisnadimide networks--products of thermal degradation and type of crosslinking points," *Polymer Degradation and Stability*, 51: 307-318 (1996).

18. Biney, Paul O., Jianren Zhou, and Laura Carson. *Praire View A&M University FAST Center Sixth Year and Final Report.* Contract F49620-95-1-0512. Praire View TX: FAST Center, August 2003 (AFRL-SR-AR-TR-03-0342).

19. Li, Yuntao. *Synthesis and Cure Characterization of High Temperature Polymers for Aerospace Applications.* PhD dissertation. Texas A&M University, College Station TX, 2004.

20. Leung, Chuk L. *Thermo-Oxidative Stability of Polyimide Composites for Aerospace Applications.* Contract F49620-95-C-0022. Washington DC : Air Force Office of Scientific Research, August 1998 (AFRL-SR-BL-TR-98-06U).

21. Biney, Paul O., Yang Zhong, and Jianren Zhou. "Hyrolytic Effects on the Properties of Graphite/BMI Composites," *43rd International SAMPE Symposium*. 120-129. Anaheim: SAMPE, 1998.

22. Bao, Li-Rong and Albert F. Yee. "Effect of temperature on moisture absorption in a bismaleimide resin and its carbon fiber composites," *Polymer*, 43: 3987-3997 (2002).

23. Schoeppner, Greg A. Air Force Research Laboratory Materials and Manufacturing Directorate, Wright-Patterson Air Force Base OH. Personal Interview. 30 April 2007.

24. Robinson,Grant W. *High Temperature Chemical Degradation of PMR-15 Neat Resins*, MS Thesis, AFIT/GAE/ENY/05-J09. School of Engineering and Management, Air Force Institute of Technology, Wright-Patterson AFB OH, June 2005.

25. Audouin, Ludmila and others. "Kinetic Modeling of Low-Temperature Oxidation of Hydrocarbon Polymers," in *Handbook of Polymer Degradation* (2nd Edition). Ed. S. Halim Hamid. Dhahran : King Fahd Institute of Petroleum & Minerals, 2000.

26. Colin, X. and J. Verdu. "Strategy for studying thermal oxidation of organic matrix composite," *Composites Science and Technology*, 65: 411-419 (2005).

27. Colin, X., "The Classical Kinetic Model for Radical Chain Oxidation of Hydrocarbon Substrates Initiated by Bimolecular Hydroperoxide Decomposition," *International Journal of Chemical Kinetics*. 38: 666-676 (November 2006).

28. Balaconis, John G. *Some Aspects of the Mechanical Response of BMI 5250-4 Neat Resin at 191^{0}C: Experiment and Modeling*, MS Thesis, AFIT/GAE/ENY/06-M03. School of Engineering and Management, Air Force Institute of Technology, Wright-Patterson AFB OH, March 2006.

29. Mendenhall, Susan P. *Thermo Gravimetric Analysis of PMR-15 Neat Resin*, MS Thesis, AFIT/GAE/ENY/04-J08. School of Engineering and Management, Air Force Institute of Technology, Wright-Patterson AFB OH, June 2004.

Vita

Ensign Patrick E. Link graduated from the University of Pennsylvania in Philadelphia, Pennsylvania in May 2006 with a Bachelor of Science degree in Mechanical Engineering and Applied Mechanics. He received his commission through the University of Pennsylvania Naval Reserve Officer Training Corps Program, and was assigned to Wright-Patterson Air Force Base to attend the Air Force Institute of Technology. After graduation in June 2007 with Masters of Science degree in Aeronautical Engineering, Ensign Link will be assigned to Naval Air Station Pensacola in Pensacola, Florida as a student naval aviator.

REPORT DOCUMENTATION PAGE	Form Approved OMB No. 074-0188

The public reporting burden for this collection of information is estimated to average 1 hour per response, including the time for reviewing instructions, searching existing data sources, gathering and maintaining the data needed, and completing and reviewing the collection of information. Send comments regarding this burden estimate or any other aspect of the collection of information, including suggestions for reducing this burden to Department of Defense, Washington Headquarters Services, Directorate for Information Operations and Reports (0704-0188), 1215 Jefferson Davis Highway, Suite 1204, Arlington, VA 22202-4302. Respondents should be aware that notwithstanding any other provision of law, no person shall be subject to an penalty for failing to comply with a collection of information if it does not display a currently valid OMB control number.
PLEASE DO NOT RETURN YOUR FORM TO THE ABOVE ADDRESS.

1. REPORT DATE *(DD-MM-YYYY)*	2. REPORT TYPE	3. DATES COVERED *(From – To)*
14-06-07	**Master's Thesis**	**Aug 2006– Jun 2007**

4. TITLE AND SUBTITLE	5a. CONTRACT NUMBER
High Temperature Degradation of 5250-4 Polymer Resin	5b. GRANT NUMBER
	5c. PROGRAM ELEMENT NUMBER
6. AUTHOR(S)	5d. PROJECT NUMBER
Link, Patrick, E., Ensign, USN	5e. TASK NUMBER
	5f. WORK UNIT NUMBER

7. PERFORMING ORGANIZATION NAMES(S) AND ADDRESS(S)	8. PERFORMING ORGANIZATION REPORT NUMBER
Air Force Institute of Technology Graduate School of Engineering and Management (AFIT/EN) 2950 Hobson Way WPAFB OH 45433-7765	AFIT/GAE/ENY/07-J12
9. SPONSORING/MONITORING AGENCY NAME(S) AND ADDRESS(ES) AFRL/ML Attn: Dr. Greg A. Schoeppner 2941 Hobson Way WPAFB OH 45433-7750 DSN: 785-9072	**10. SPONSOR/MONITOR'S ACRONYM(S)** **11. SPONSOR/MONITOR'S REPORT NUMBER(S)**

12. DISTRIBUTION/AVAILABILITY STATEMENT
APPROVED FOR PUBLIC RELEASE; DISTRIBUTION UNLIMITED.

13. SUPPLEMENTARY NOTES

14. ABSTRACT

5250-4 bismaleimide resin is used in high performance polymer matrix composites with high temperature aeronautical applications. This thesis investigated the thermal and oxidative degradation of 5250-4 neat resin powder in argon, air, and oxygen environments. The powder was aged at 163, 177, and 190 ^{0}C in all environments for at least 250 hours. Isothermal thermo-gravimetric analysis demonstrated that weight loss was negligible for aging in the argon environment, indicating weight loss is the result of an oxidative process at these temperatures. The 5250-4 powder exhibited an initial period of weight gain before eventually losing weight in both air and oxygen. The applicability of a closed loop oxidation scheme to 5250-4 gravimetric behavior was investigated. Kinetic parameters for the scheme were determined for the Air Force Research Laboratory's polymer matrix composite lifetime prediction modeling efforts.

15. SUBJECT TERMS
Thermogravimetric Analysis, Composite Materials, Thermal Degradation, Matrix Materials, Thermo-Oxidative Aging

16. SECURITY CLASSIFICATION OF:			17. LIMITATION OF ABSTRACT	18. NUMBER OF PAGES	19a. NAME OF RESPONSIBLE PERSON
REPORT	ABSTRACT	c. THIS PAGE			Dr. Anthony N. Palazotto (AFIT/ENY)
U	**U**	**U**	**UU**	99	**19b. TELEPHONE NUMBER** *(Include area code)* (937) 255-6565, e-mail: Anthony.palazotto@afit.edu

Standard Form 298 (Rev: 8-98)
Prescribed by ANSI Std. Z39-18